THE 'SOURCES' OF PLASMA PHYSICS

Francis F. Chen

Electrical Engineering Department

PPG- 1521 October, 1994

Submitted to IEEE Transactions on Plasma Science.

THE 'SOURCES' OF PLASMA PHYSICS

Francis F. Chen

University of California, Los Angeles, CA 90024-1594

ABSTRACT

This paper is the text of the Plasma Science and Applications Committee Prize address given in Santa Fe, NM on June 7, 1994. The principal thesis is that major advances in the development of the science of plasmas have frequently been triggered by the invention of a new plasma source. Examples are given from the work of many colleagues in basic plasma research. A retrospective of the author's experiments on basic plasma physics, magnetic fusion, and inertial fusion is given, many of these sharing the common theme of transverse electric fields. The author's present and future work concern new plasma sources that are needed for the application of plasma technology to materials processing.

THE 'SOURCES' OF PLASMA PHYSICS

Francis F. Chen

University of California, Los Angeles, CA 90024-1594

I. INTRODUCTION

The science of plasmas has grown enormously over the past forty years, and the key to the expansion of our knowledge about plasma behavior has been the discovery of new, better ways to create plasmas. The development of basic plasma physics can actually be traced through the invention of new sources, which each time triggered new insights into the behavior of plasmas. In Sec. II, I shall give a number of examples of such break-through plasma sources and the classic experiments that resulted from them. This section will include not only my own work but also that of others. I take this opportunity to honor my colleagues who, over the years, have joined me in the mission to establish and solidify the foundations of plasma physics through inspired experimentation. In Sec. III, I shall discuss a number of experiments, mostly my own, including unpublished ones, which are tied together through a common theme, that of transverse electric fields. Finally, Sec. IV will project what the technological plasma sources of the future will do for our science.

II. BREAK-THROUGH PLASMA SOURCES

1. Duoplasmatron source. Figure 1 shows the Duoplasmatron source of Boeschoten and Schwirzke[1]. The plasma is created in a small filament discharge at 40 mTorr of H and injected through a 1-3 mm diam hole through a magnetic mirror into the main chamber, which is 120 cm long, with a magnetic field of up to 4 kG and pressures as low as 10^{-5} Torr. The small-diameter plasma was quiescent enough for basic experiments on electrons. No one knows why the plasma was more stable than in other sources; perhaps it was ion FLR stabilization or favorable curvature in the source region. The most famous result arising from this source is, of course, Malmberg and Wharton's demonstration of electron Landau damping[2]. This was reported at the IAEA meeting in London in the early '60s, and the familiar result is shown in Fig. 2. The amplitude Fig. 1 was shown to decay exponentially as predicted. Up to this time there was doubt as to whether Landau damping was a real effect, since it was not clear that electrons could follow a Maxwellian distribution as closely as the theory required; that they do so is still a puzzle, called Langmuir's paradox. This experiment was an important demonstration, and it succeeded because the duoplasmatron source could provide a suitable plasma.

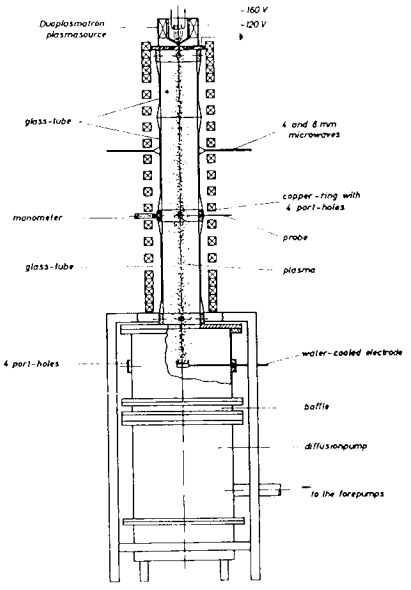

Fig. 1. The duoplasmatron source (Ref. 1).

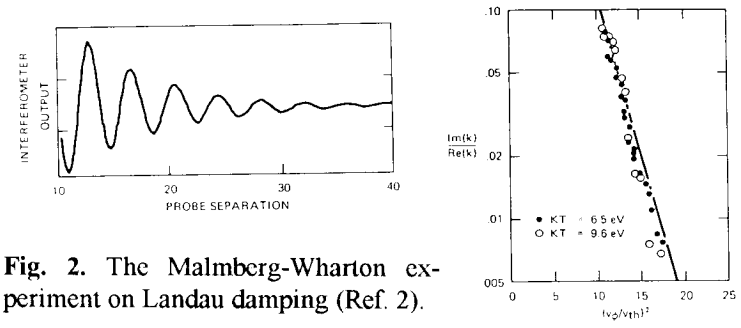

Fig. 2. The Malmberg-Wharton experiment on Landau damping (Ref. 2).

2. The "hot-house" discharge.

The first verification of Alfvén waves was made possible by a very special plasma which could produce 10^{15} cm^{-3} densities in hydrogen at 10 kG. This was the "hot-house" discharge, or slow pinch, developed by Bill Baker at Berkeley using a slow capacitor bank to drive a current between two endplates without actually pinching the plasma. Torsional Alfvén modes were excited with a ringing capacitor bank applied between a central electrode and the wall. The high density was necessary to slow down the wave to fit inside the chamber, and the high magnetic field and light ion mass were necessary to minimize the damping. Figure 3 from the paper of Wilcox et al.[3] shows that producing a good plasma was not simple; instabilities would occur without certain modifications. Figure 4 shows the experiment of Wilcox, Boley, and deSilva[4] et al. verifying the constancy of the Alfvén velocity. A similar experiment was also done in England by Jephcott.

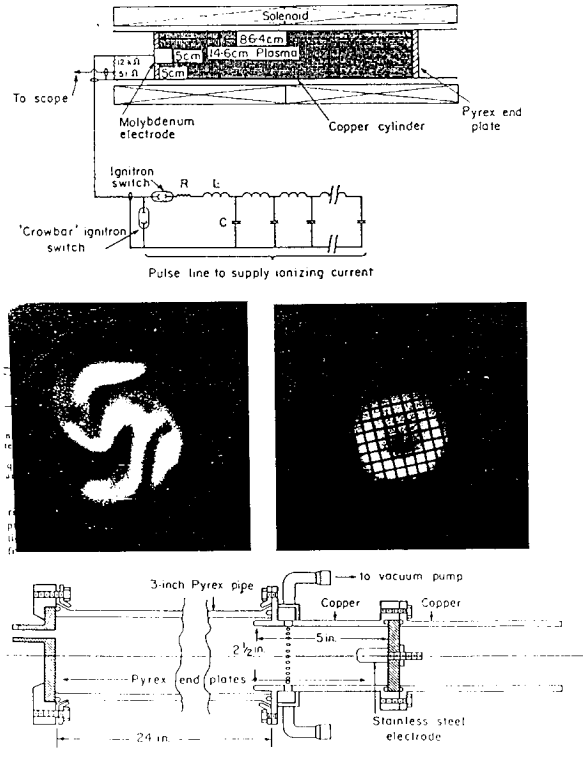

Fig. 3. The "Hot house) discharge (Ref. 3).

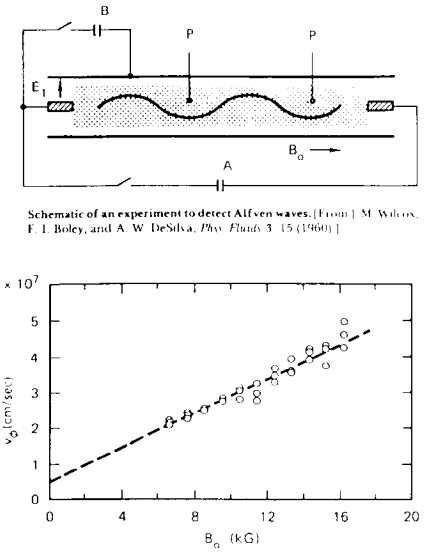

Schematic of an experiment to detect Alfven waves. [From F. M. Wilcox, F. I. Boley, and A. W. DeSilva, *Phys. Fluids* 3, 15 (1960).]

Fig. 4. Detection of Alfven waves (Ref. 4).

3. The double-plasma device. Experimental nonlinear plasma physics had its roots in the invention of the double-plasma machine by Taylor, MacKenzie, and Ikezi[5]. By separating two filament discharges with a grid and applying a bias voltage between the two chambers, one can cause plasma to stream from one discharge into the other at velocities exceeding the

sound velocity. Ion acoustic shock waves could be studied for the first time. The device is shown in Fig. 5, and the classic shock wave structure predicted by Sagdeev, as measured by Taylor, Baker, and Ikezi[6], is shown in Fig. 6.

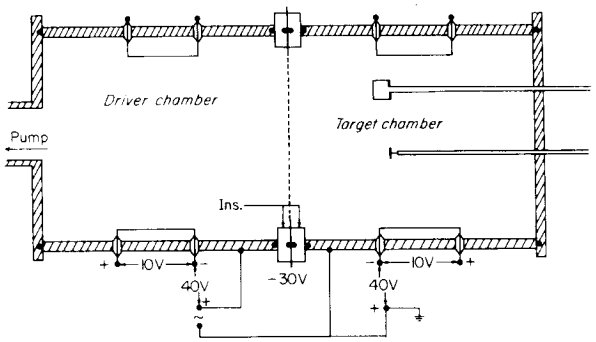

Fig. 5. The double-plasma device (Ref. 5).

Double and triple plasmas have since been used to see such phenomena as solitons and double layers, the latter of importance in ionospheric physics. Fig. 7 shows the collision (or lack of one) of two Korteweg-deVries solitons seen by Nakamura and Tsukabayashi[7], and Fig. 8 shows the distribution functions measured by Quon and Wong[8] in various parts of a double layer produced in a triple plasma system.

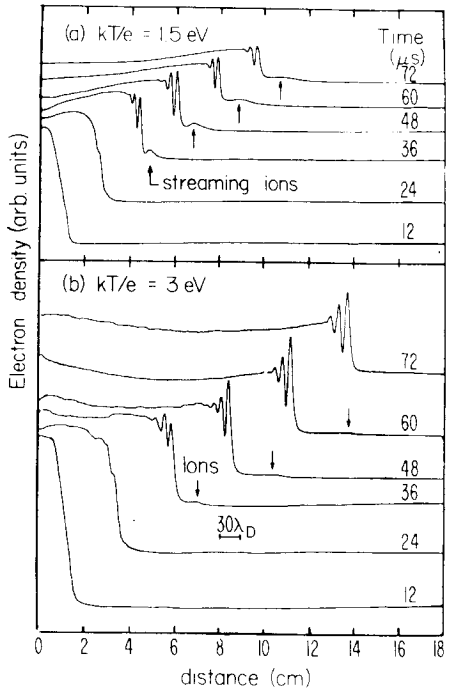

Fig. 6. Observation of ion acoustic shock waves (Ref. 6).

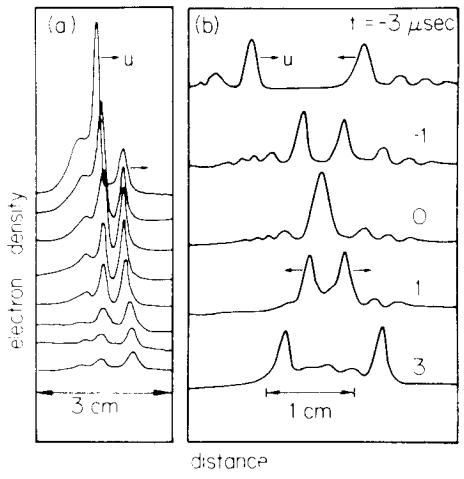

Fig. 7. Collision of solitons (Ref. 7).

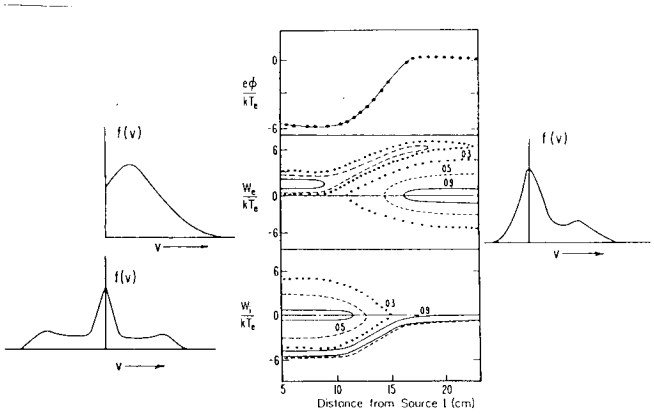

Fig. 8. Distribution functions in a double layer (Ref. 8).

A very small double plasma was used by Ripin and Stenzel[9] to excite Bernstein waves with an ion beam. The apparatus is shown in Fig. 9, and the dispersion relation check in Fig. 10. This experiment also demonstrated the phenomenon of backward waves. Fig. 11 shows the interferometer wave pattern, which has an amplitude modulation. The wave phase velocity and the group velocity of the envelope were directly seen to move in opposite directions, in agreement

with the negative slope of Fig. 10. These plasma devices have played an essential role in our understanding of basic plasma phenomena.

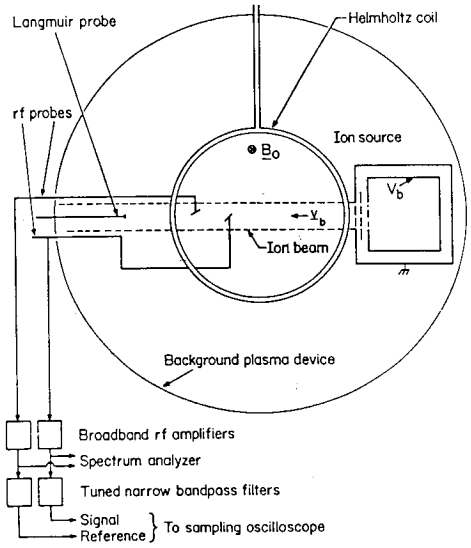

Fig. 9. Electron cyclotron drift wave experiment using a double plasma (Ref. 9).

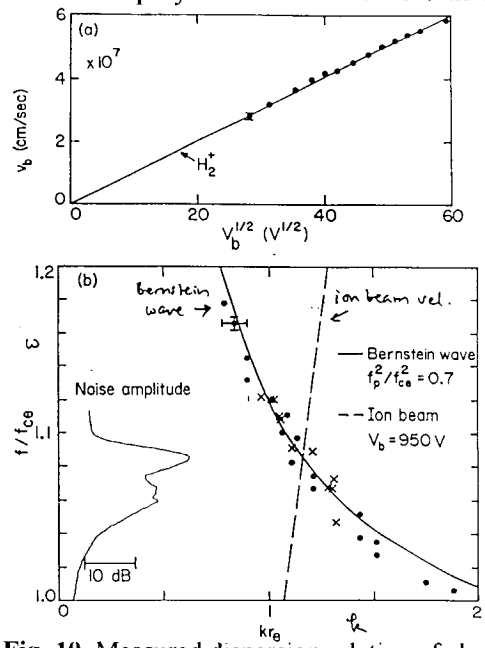

Fig. 10. Measured dispersion relation of electron Bernstein wave (Ref. 9).

4. The MacKenzie bucket. Though not a plasma source in itself, the multi-dipole confinement scheme using permanent magnets around the surface of a plasma has improved the performance of many plasma sources by confining the primary electrons while keeping the plasma field-free in the interior. Neutral beam injectors for tokamaks, for instance, depend on this device, as do several etching and deposition tools used in the semiconductor industry. Story has it that Ken MacKenzie made the first one of these at UCLA using a surplus Navy soup pot, which not only was made of stainless steel, but also had walls thin enough that the magnets could be put on the outside. Fig. 12 shows a modern version of the MacKenzie bucket.

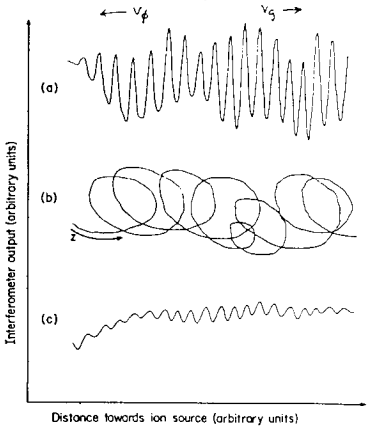

Fig. 11. Demonstration of backward waves (Ref. 9).

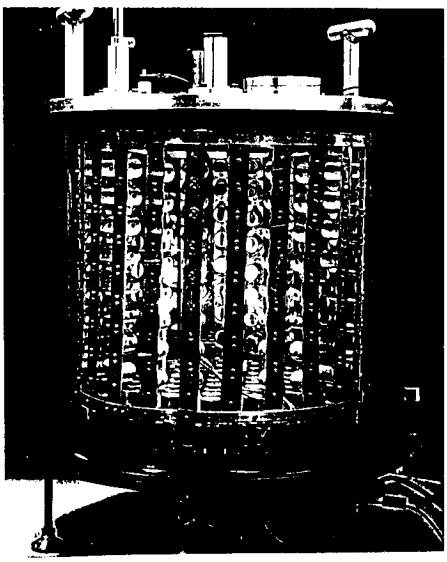

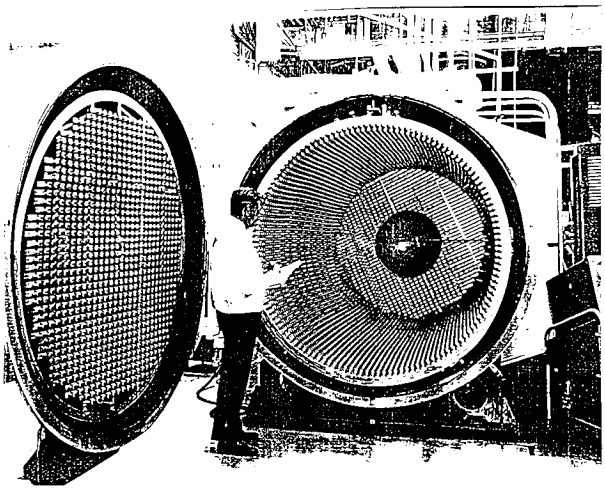

Fig. 12 (previous page). A multidipole confinement chamber [R. Limpaecher and K.R. MacKenzie, Rev. Sci. Instrum. 44, 726 (1973), courtesy of R.L. Stenzel].

Fig. 14. (previous page). A large-cathode plasma source with multidipole confinement (R.L. Stenzel, private communication).

5. Large area cathode discharge. For detailed probing of a plasma, no source is better than the hot-cathode discharge developed by Stenzel[10], shown in Fig. 13. The oxide-coated cathode is stretched flat with springs and indirectly heated by filaments behind it. The emitted electrons are accelerated through a pulsed anode grid and confined radially by a weak magnetic field and axially by a multi-cusp magnet array. Stenzel and Gekelman have refined the cathode design until it can give a uniform plasma over a large volume of order 1m in diam and 4m long. Many probes of different varieties can be inserted without disturbing the large plasma. The magnetic field, however, is limited to about 800 G; otherwise, the plasma is subject to drift-wave instabilities when FLR or viscous stabilization is no longer effective.

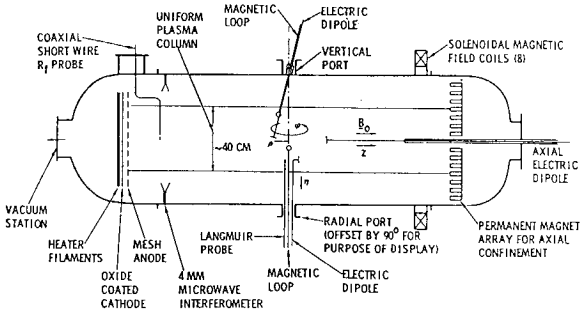

Fig. 13. Diagram of a large-area, hot-cathode plasma source (Ref. 10).

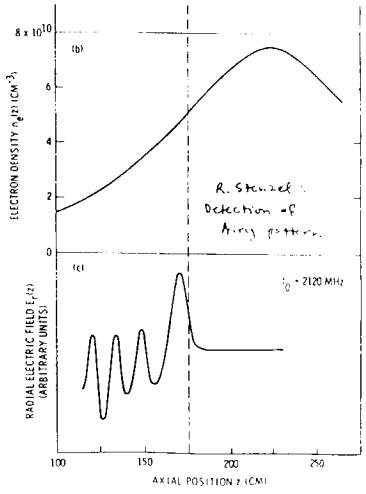

Fig. 15. Detection of Airy pattern formed by electromagnetic waves in a nonuniform plasma (Ref. 11).

Fig. 14 shows the QUIPS device built at TRW, Inc.; this has multi-cusp confinement on all walls. By purposely creating an axial density gradient, Stenzel[10] demonstrated for the first time the Airy pattern that electromagnetic waves were predicted to generate when they impinge on a nonuniform plasma (Fig. 15). Stenzel's[11] investigation of whistler waves was done in another large chamber (Fig.16) with a uniform dc magnetic field. This experiment graphically illustrated concept of group velocity in an anisotropic medium. Fig. 17a shows the phase fronts of a whistler wave, laboriously mapped out with probes. At each point the phase velocity direction is perpendicular to the phase fronts, and the group velocity could be calculated theoretically from the θ dependence of the index of refraction. The resulting arrows in Fig. 17b give the group velocity directions, and indeed the wave amplitude was found to maximize in the direction of energy flow. This experiment

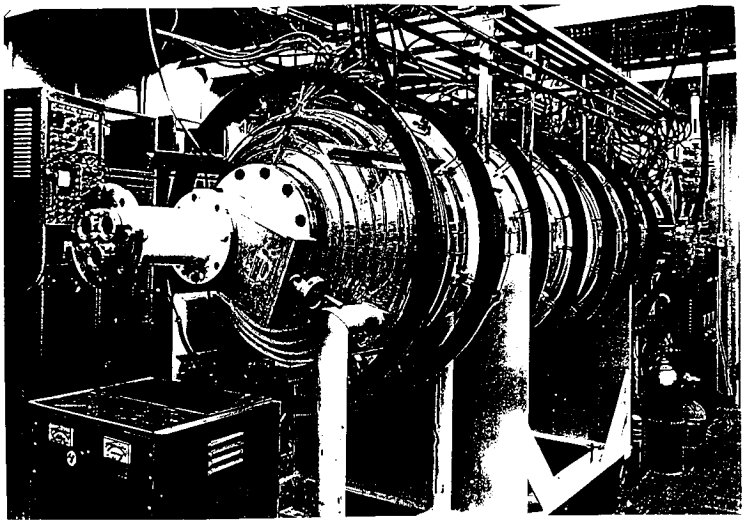

also established the space-relevant concept of nonlinear ducting, in which a wave traps itself in a density trough that it digs by its radiation pressure (Fig. 18).

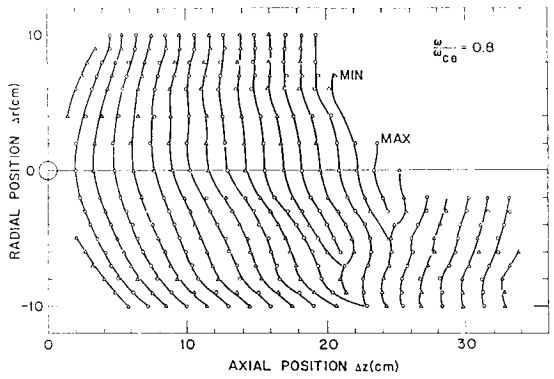

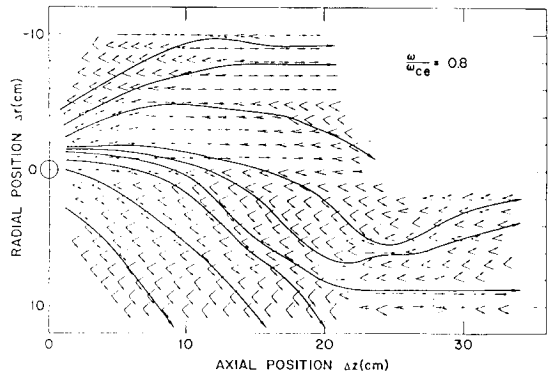

Fig. 17. Whistler wavefronts (a) and phase and group velocity directions (b) (Ref. 10).

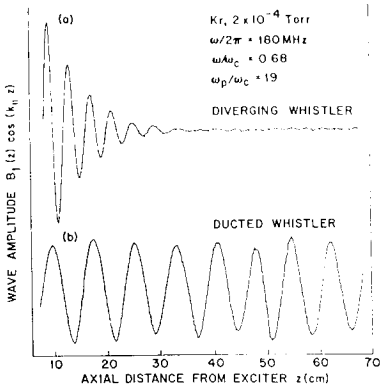

Fig. 18. Demonstration of ducted whistler waves (Ref. 10).

Because of the large plasma volume, field annihilation could be studied in detail for the first time. Fig. 19 shows the magnetic field pattern in a tearing instability[12]. By this time data acquisition and analysis by computers had advanced so that the three-dimensional distribution functions at every point in this pattern could be measured and shown in a movie[13]. The simple conduction of current through a plasma turned out to be nontrivial. By applying a fast-rising pulse between the cathode and a collector at the far end of the discharge, Stenzel et al.[14] flows at first backward toward the endplate, and only reaches the far end after a whistler-wave time of flight (Fig. 20a). The current generates its own magnetic field and falls into a force-free configuration called a flux rope (Fig. 20b).

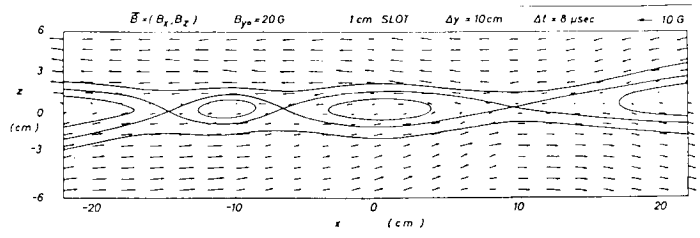

Fig. 19. Magnetic field lines in reconnection and tearing (Ref. 14).

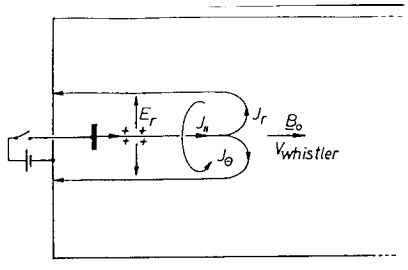

Fig. 20. Initial path of a pulsed current in a plasma (Ref. 14).

Fig. 21. Self-distortion of a current path into a flux rope (Ref. 14).

Walter Gekelman has extended the large-cathode technique to even larger plasmas, using an improved cathode structure. Fig. 22 shows his LAPD device, which produces a plasma 50 cm in diam by 10 m long in a magnetic field of up to 3 kG. With probes designed to cover the entire plasma, he has been able to simulate whistler and Alfvén wave propagation in density channels, and other phenomena such as the interaction of current filaments[15] (Fig. 23).

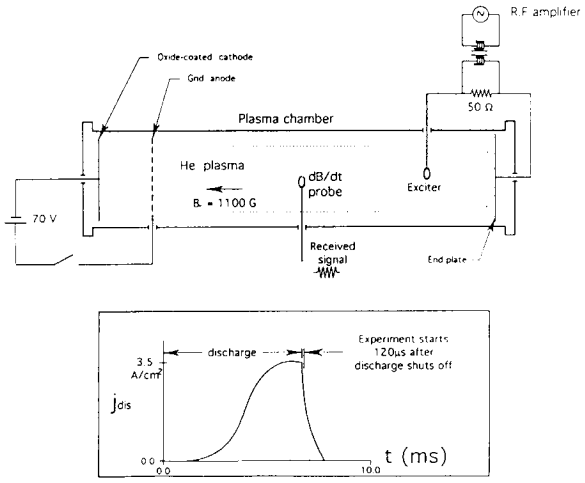

Fig. 22. Schematic of the Large Area Plasma Device (Ref. 15).

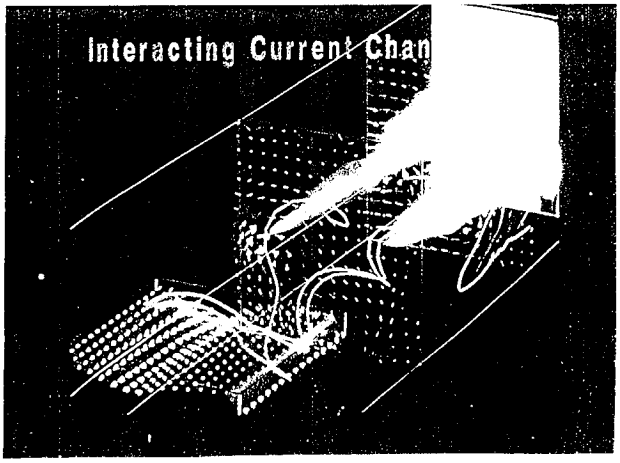

Fig. 23. Interaction of current filaments in the LAPD machine (Ref. 15).

6. Q-machines. Though it is clear that the plasma sources described above have yielded a rich variety of interesting results, perhaps the most significant and important discoveries followed the invention of the Q (for Quiescent) machine. The noise level of these plasmas was low enough that, for the first time, delicate effects like universal instabilities could be seen, and this discovery ultimately had a great influence on our understanding of anomalous diffusion. Fig. 24 is an enlargement of from the paper of Rynn and D'Angelo[16], a diagram that was a mere 1½ inches wide in the original. Fig. 25 shows how it works.

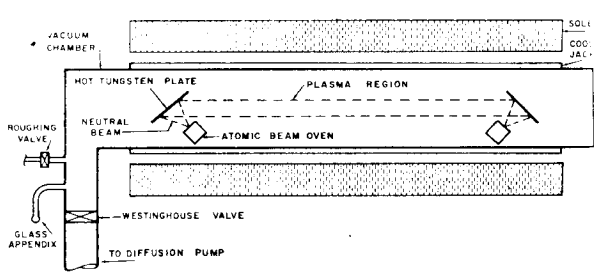

Fig. 24. Original diagram of the Q-machine (Ref. 16).

The plasma is synthesized by the injection of electrons which are thermionically emitted by tungsten "cathodes" heated to ≈2400°K by electron bombardment, and of ions which are contact-ionized from neutral beams of cesium, potassium, or barium produced in 400°C ovens. These metals have such low ionization potentials that when an atom impinges on a high work function material like tungsten or molybdenum, an electron is drawn into the metal, and a singly ionized ion is emitted. The plasma is held together by a strong axial magnetic field. Both species have the same temperature as the cathodes, just above 0.2 eV. Since no voltages are applied to the plasma, there are few energy sources which can excite instabilities; and a quiescent plasma can be produced. Actually, there *is* an applied voltage; namely, the contact potential of several volts between the hot cathodes and the cold stainless steel walls, but this can be controlled by floating the vacuum chamber and

applying a bias voltage V_c, as shown in Fig. 25. Fig. 26 shows radial profiles of the probe floating potential V_f and the plasma density ($\propto J_+$) in a typical Q-machine. Also shown are oscillation amplitudes of noise around 4 kHz and 15 kHz when $V_c = 0$ and the magnetic field B_0 is above about 2 kG. The former peaks near the maximum of $\tilde{n}$ and is due to drift waves; the latter peaks near the maximum of E_r and has been identified as a Kelvin-Helmholtz instability. Identification of the low-frequency oscillations as resistive drift waves was made by Hendel, Chu, and Politzer[17], whose famous graph showing the onset of higher azimuthal m modes with increasing B_0 is shown in Fig. 27. The stability at low fields is attributed to viscous damping by the ions when their Larmor radii become large.

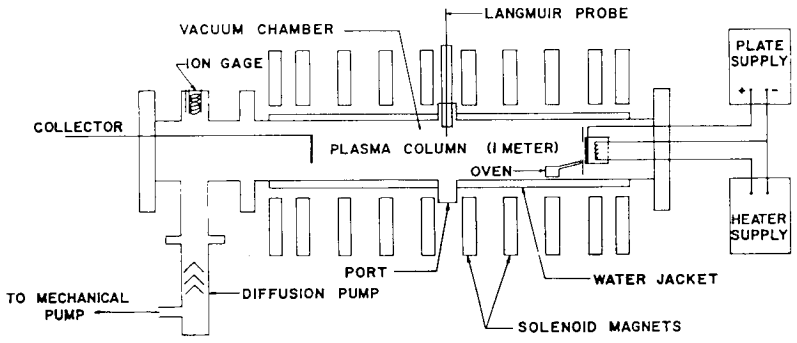

Fig. 25. Operation of a single-ended Q-machine (Ref. 16).

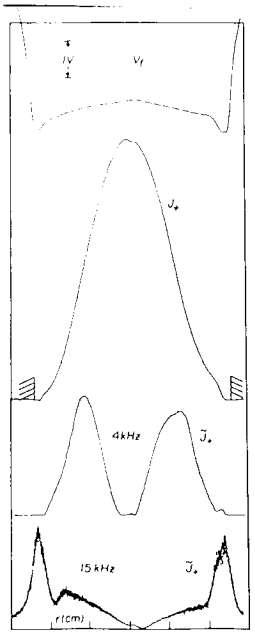

Fig. 26. Typical radial profiles of floating potential V_f, ion saturation current J_+, and drift-wave and Kelvin-Helmholtz wave amplitudes in a Q-machine.

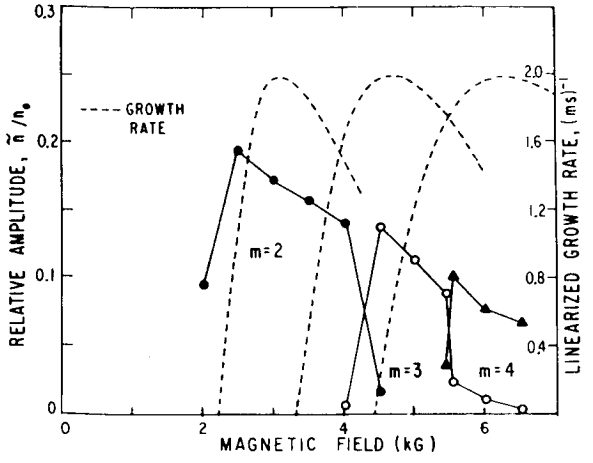

Fig. 27. Threshold behavior of drift-wave modes in a Q-machine (Ref. 17).

The discovery and exploration of drift waves is perhaps the most important advance in plasma physics that is attributable to a new plasma source. Until a zero-order density gradient was put into the theory of plasma waves, we had no idea of why the fluctuation spectrum was peaked in the 10-kHz range and what it had to do with anomalous transport. Though collisionless drift waves (universal instabilities) had been found by theorists, they were buried among many predictions, most of which turned out to be unimportant in the real world. The observation of low-frequency instabilities in Q-machines, which had no source of free energy other than the pressure gradient present in any confined plasma, focused attention on dissipative drift waves triggered by resistivity or trapped particles. Even today, 30 years after the initial excitement, drift wave turbulence is still at the forefront of tokamak confinement research.

The Q-machine also opened our eyes to other phenomena, such as electrostatic ion cyclotron waves. By drawing a current along the axis of the plasma, Motley and D'Angelo[18] saw, for the first time, unstable waves at the ion cyclotron frequency propagating across the

magnetic field (Fig. 28). This instability is important because it usually has a lower threshold than the ion acoustic instability, which theorists have studied *ad infinitum* but which is hardly ever observed.

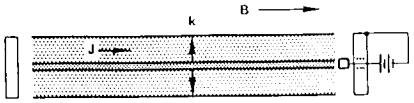

Schematic of a Q-machine experiment on electrostatic ion cyclotron waves. [After R. W. Motley and N. D'Angelo, *Phys. Fluids* 6, 296 (1963).]

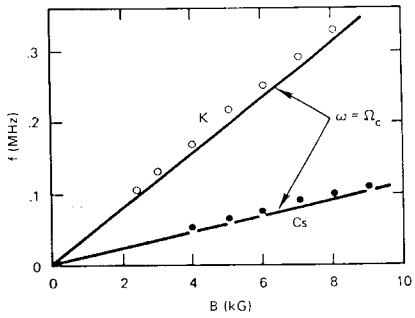

Fig. 28. Experiment for generating electrostatic ion cyclotron instability (Ref. 18).

The Q-machine also allowed Wong, Motley, and D'Angelo[19] to verify, for the first time, the existence of ion acoustic waves, which, though well known in theory, had been impossible to see in noisy plasmas. Fig. 29 shows their single-ended Q-machine, and Fig. 30 their check of the basic dispersion relation. They also measured the damping in the upstream and downstream directions, as shown in Fig. 31, thereby [16]establishing the validity of ion Landau damping. This work actually preceded the experiment of Malmberg and Wharton, so that *ion* Landau damping provided our first indication that collisionless damping was real.

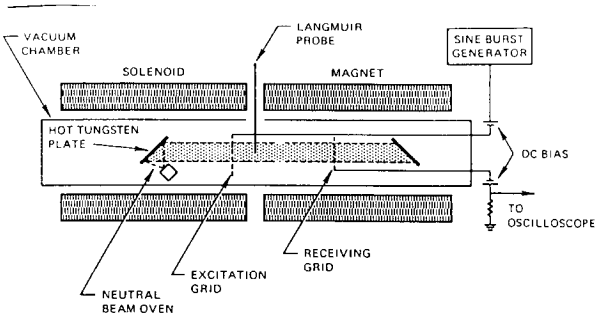

Fig. 29. Q-machine used for verification of ion acoustic waves (Ref. 19).

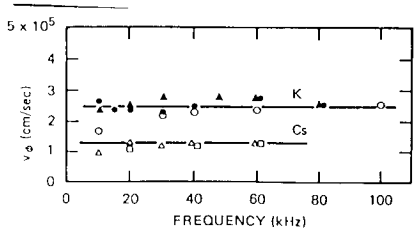

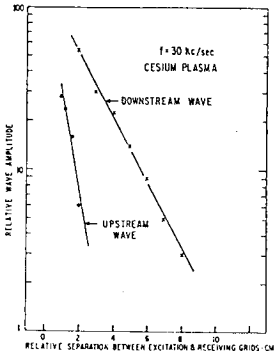

Fig. 30. Measured ion acoustic dispersion relation (Ref. 19).

Fig. 31. Damping of ion acoustic waves (Ref. 19).

The Malmberg-Wharton experiment on electron Landau damping was later refined using a Q-machine by Barrett, Jones, and Franklin[20] with smaller values of $k\lambda_D$, where the damping was quite weak, and the damping rate was more difficult to measure. Their signals at various densities are shown in Fig. 32, where it is shown that sometimes the apparent damping is not due to Landau damping at all but to phase mixing caused by noise in Q-machines at low densities.

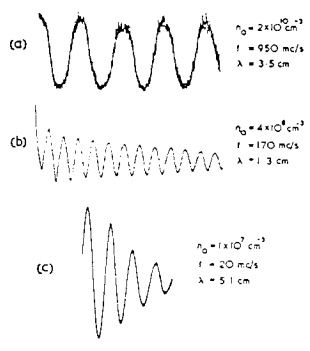

Fig. 32. Spurious electron Landau damping due to noise (Ref. 20).

7. Multipoles. Though these machines were spawned by fusion research rather by basic plasma research, we should not leave unmentioned such devices as multipoles, spherators, and levitrons, which also produced quiescent plasmas. With the help of floating

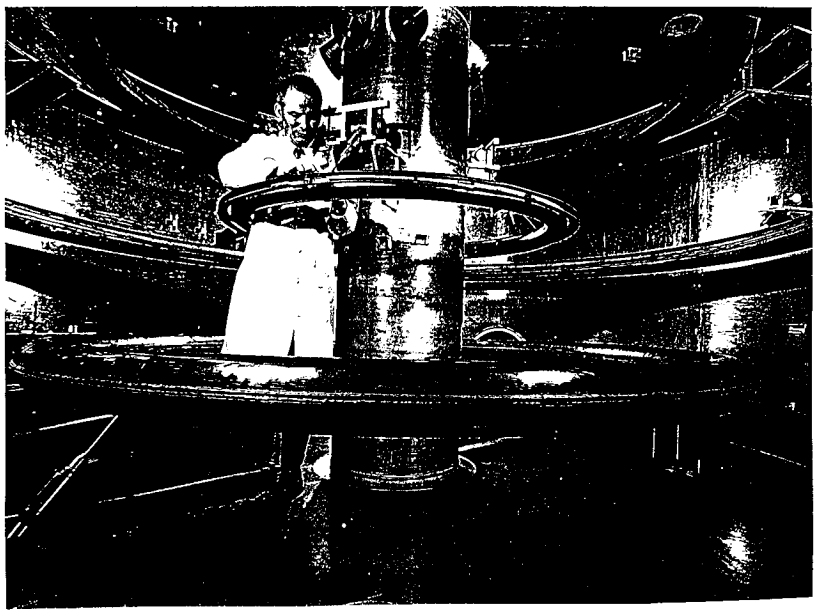

Fig. 33. The octopole machine at GA. [F.F. Chen, *Intro. to Plasma Physics*, 1st ed. (1973).]

internal conductors, these devices could create a magnetic well and prove the principle of minimum-average-B stabilization. The two largest machines were Tihiro Ohkawa's octopole at General Atomics and Don Kerst's octupole at Wisconsin. I remember when the picture of a man standing inside the octopole (Fig. 33) was shown at the IAEA conference in Novosibirsk in 1968. The Russians were astounded that the US had the means to build a fusion machine that large, until they realized that the magnetic field was only 150G! The plasma produced was so quiescent that cross-field diffusion at the classical rate was observed here for the first time.

8. Laser-ionized plasmas. The birth of parametric instabilities and laser-plasma interactions can be traced to the summer of 1973, when a surge of activity produced the main theoretical predictions on stimulated the Brillouin (SBS) and Raman (SRS) instabilities. To verify these phenomena, which occurred all at once in solid targets, it was necessary to design plasma sources, used as targets, which could permit the instabilities to be observed one at a time. The critical density for a CO_2 laser is 10^{19} cm^{-3}, and we needed a density that was a non-negligible fraction of this but not as high as ¼ of it, so as to avoid resonant layers. The first device we tried was a high-current arc, shown in Fig. 34, with holes in the anode and cathode for laser beam access. This produced densities in the 10^{16}-10^{17} cm^{-3} range and permitted us[21] to observe pure SBS, uncontaminated by other effects, showing its anomalously low saturation level (Fig. 35). We found later[22] that the arc provided only part of the ionization; the laser pulse itself completed the ionization and formed a cigar-shaped region of uniform plasma, as shown in the interferogram of Fig. 36. Nonetheless, preionization by the plasma source was absolutely necessary to produce a uniform, reproducible, and jitterless plasma target.

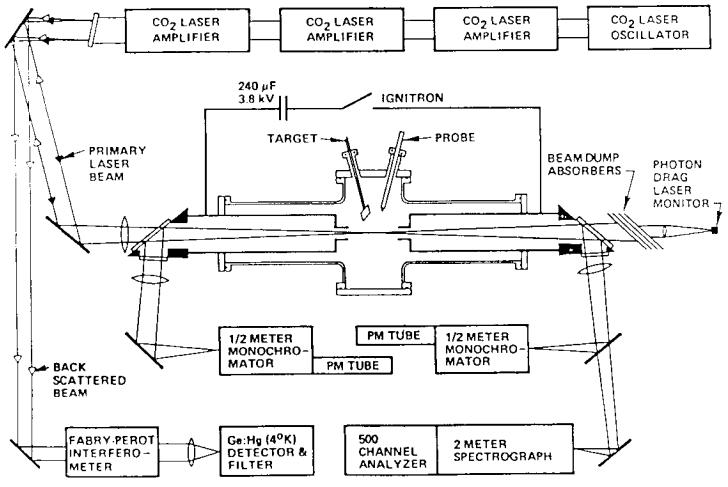

Fig. 34. High current arc used for laser-plasma interaction experiments (Ref. 21).

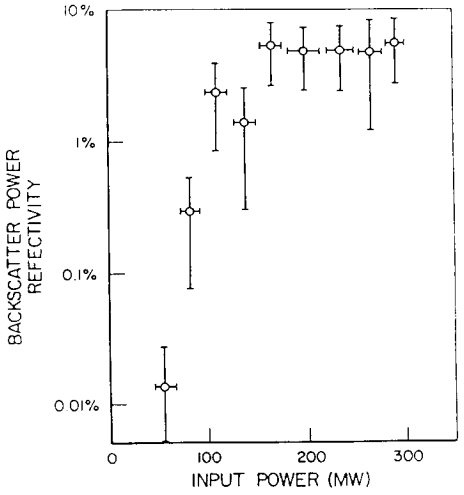

Fig. 35. Saturation level of stimulated Brillouin instability (Ref. 22).

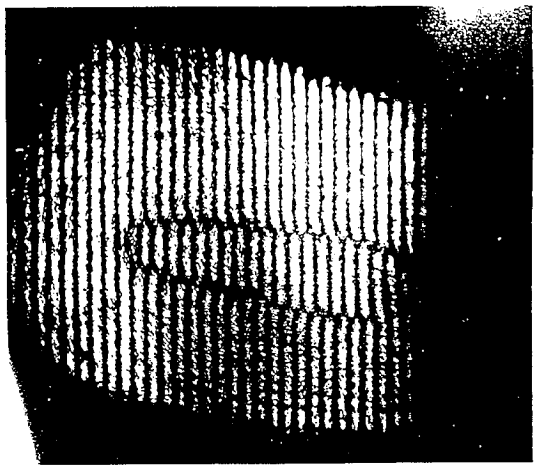

Fig. 36. Side-on interferogram showing density uniformity in laser-heated plasma (Ref. 22).

The next problem was to isolate the SRS instability. Since SBS has a lower threshold, we had to devise a plasma source to suppress SBS. We used a slow theta pinch, shown in Fig. 37. This had good axial access; the plasma at maximum compression (Fig. 38) was uniform; the density was around 10^{17} cm^{-3}; and, most important, the ions were hotter than the electrons, thus Landau damping the ion waves that SBS generates. This source allowed us to observe pure SRS and verify its anomalously low threshold[23]. We also used the theta pinch to demonstrate beat-wave excitation of plasma waves with counter-propagating beams[24]. Fig. 39 shows the set-up, and Fig. 40 shows the Thomson-scattering peak when the plasma frequency matched the difference frequency of the two laser beams. Beat frequency coupling with co-propagating beams had been done on the high-current arc[25]. The theta pinch was also used initially as the plasma source for beat-wave accelerator experiments (Fig. 41). However, it turned out that small irregularities in the large magnetic field of the pinch disturbed the electron optics, and what is being used now is a small variant of the high-current arc with tunneling ionization by the laser to complete the process. The use of gas targets produced by specially designed plasma sources permitted us to check theory and find the holes in it, thus solidifying the foundations of laser interactions.

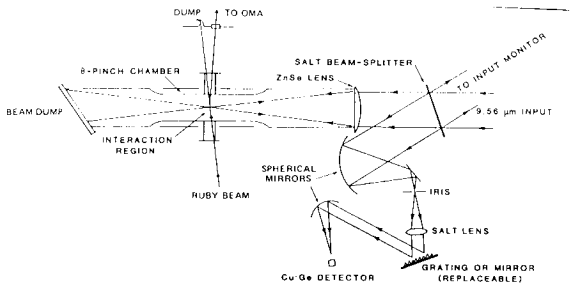

Fig. 37. Theta-pinch plasma source set up for SRS experiment (Ref. 23).

Fig. 38. End-on interferogram showing density uniformity in theta-pinch plasma (Ref. 23).

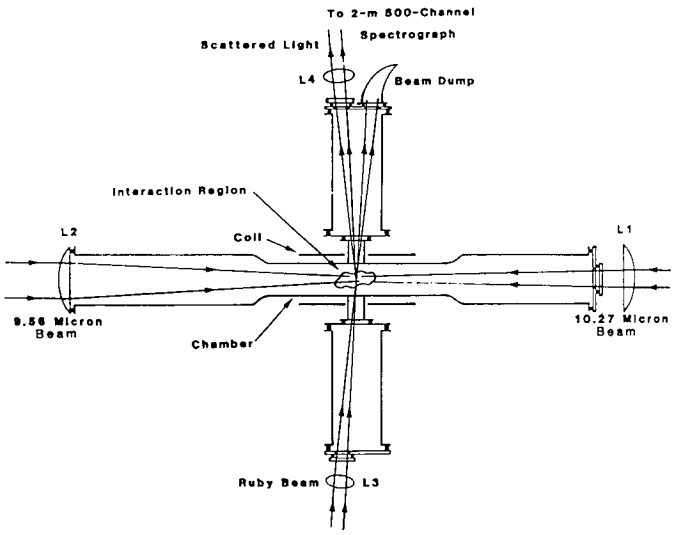

Fig. 39. Theta-pinch plasma source set up for counterstreaming beat wave experiment (Ref. 24).

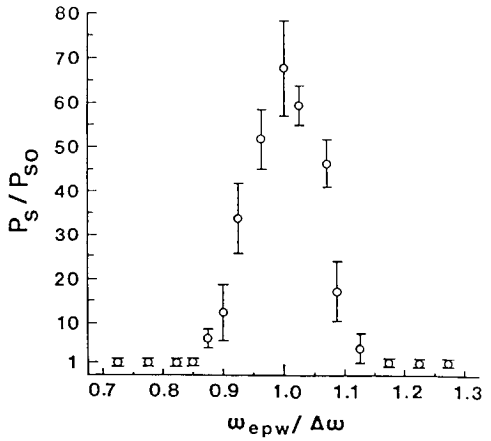

Fig. 40. Thomson scattering signal showing density resonance in beat-wave excitation (Ref. 24).

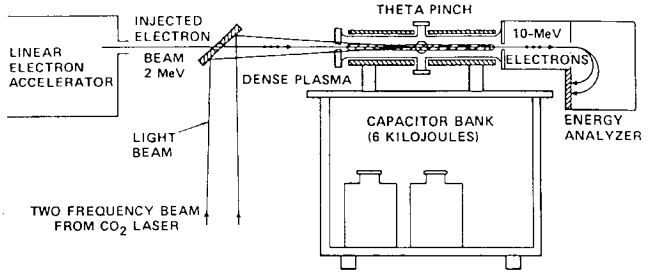

Fig. 41. Theta pinch set up for beat-wave accelerator experiment.

III. TRANSVERSE ELECTRIC FIELDS

We now move on to a group of experiments, mostly my own, which are related by a common theme: transverse electric fields. These fields have recently come into prominence because of the importance of edge layer physics in the tokamak H-mode, but the importance of transverse E-fields and my interest in them started more than 30 years ago. The H-mode itself may be considered a new break-through plasma source for investigating these fields!

1. The reflex arc. Before the invention of the Q-machine, we were searching for a plasma source that could provide a uniform, quiescent plasma in a strong, uniform magnetic field. My idea was that we had no hope of understanding anomalous transport in complicated magnetic geometries unless we first understood it in a straight geometry. The Lehnert-Hoh experiment[26] had already shown the validity of this approach, but we had to do it in a plasma that was not collision-dominated. I believe that Lyman Spitzer never forgave me for forsaking the stellarator, but at least he listened to reason and permitted me first to construct a small reflex arc L-1, and then to plan a basic research program around a large reflex arc, L-2. Fig. 42

shows an engineering drawing of L-2, and Fig. 43 a picture of it. The machine was designed by Joe File and Wendy Lehmann[27]. I understand that Joe has recently retired from Princeton; and Wendy, you may not know, is one of the founders of Princeton Applied Research, the makers of lock-in amplifiers that has since been absorbed by EG&G.

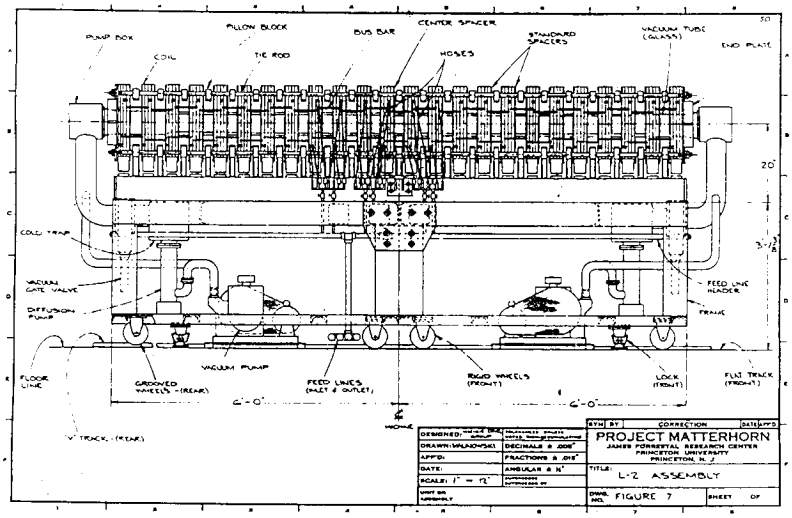

Fig. 42. Design drawing of the L-2 machine (Ref. 27).

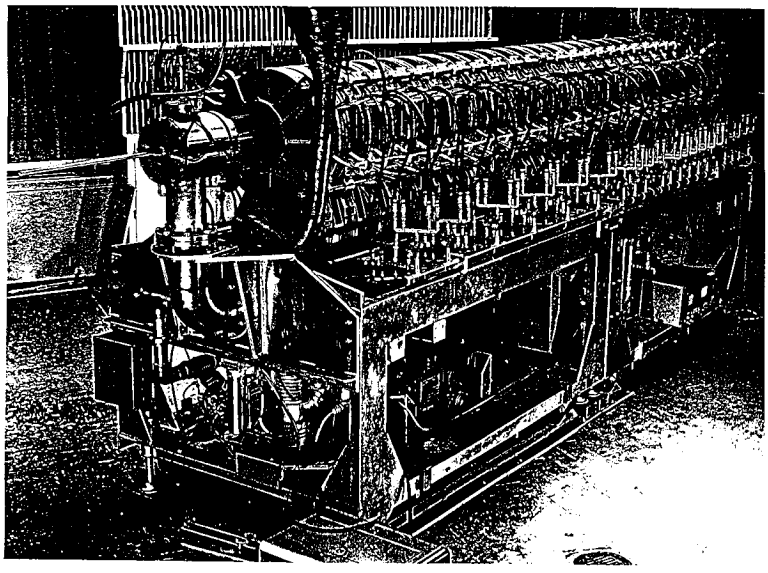

Fig. 43. The L-2 machine with the hard core installed (Ref. 27).

The L-2 coil system is 12 feet long, the length dictated by the half-wavelength of Alfvén waves that we had hoped to generate at the fields and densities achievable. When the coils are arranged in groups of four, with an equal length of gap for diagnostic access, the maximum field is 4 kG. The machine was later converted into a Q-machine and then dismantled after 1969. The L-2 coils, however, seem to have a life of their own and will probably outlive all of us. First used at Princeton for the ACT-1 machine, the coils are now dispersed all over the country, serving experiments at North Carolina, Wisconsin, and UCLA Physics.

The L-2 reflex arc used hot cathodes, four-inch diam slabs of tungsten heated by electron bombardment to 2400°K. The filaments emitting the bombardment current were pre-bent

shows an engineering drawing of L-2, and Fig. 43 a picture of it. The machine was designed by Joe File and Wendy Lehmann[27]. I understand that Joe has recently retired from Princeton; and Wendy, you may not know, is one of the founders of Princeton Applied Research, the makers of lock-in amplifiers that has since been absorbed by EG&G.

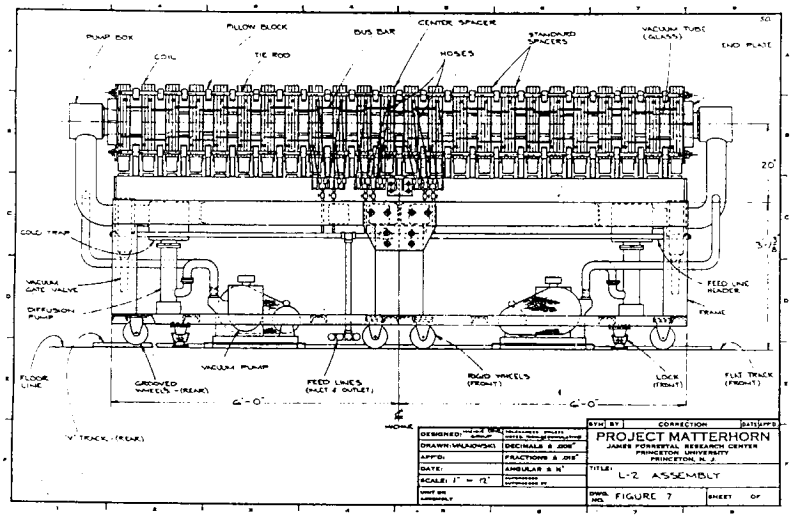

Fig. 42. Design drawing of the L-2 machine (Ref. 27).

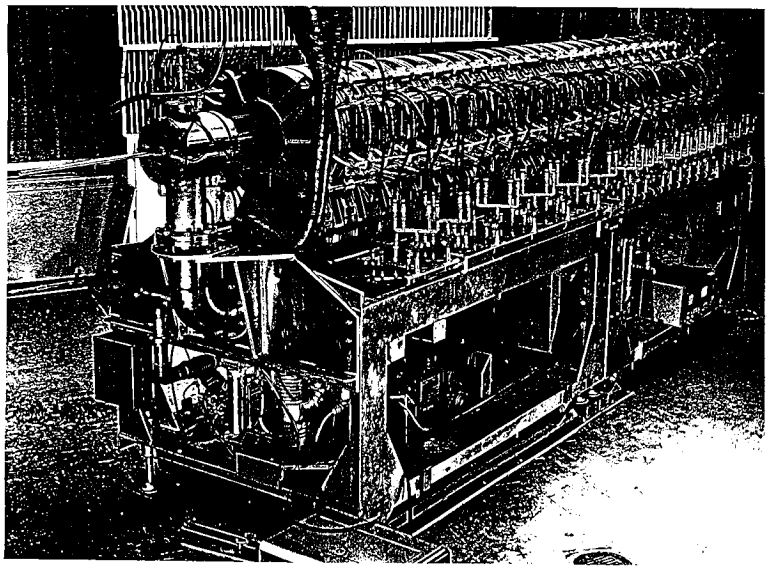

Fig. 43. The L-2 machine with the hard core installed (Ref. 27).

The L-2 coil system is 12 feet long, the length dictated by the half-wavelength of Alfvén waves that we had hoped to generate at the fields and densities achievable. When the coils are arranged in groups of four, with an equal length of gap for diagnostic access, the maximum field is 4 kG. The machine was later converted into a Q-machine and then dismantled after 1969. The L-2 coils, however, seem to have a life of their own and will probably outlive all of us. First used at Princeton for the ACT-1 machine, the coils are now dispersed all over the country, serving experiments at North Carolina, Wisconsin, and UCLA Physics.

The L-2 reflex arc used hot cathodes, four-inch diam slabs of tungsten heated by electron bombardment to 2400°K. The filaments emitting the bombardment current were pre-bent

in the direction of the **j** × **B** force so as to maintain their shape at all magnetic fields[28]. The two cathodes are connected together and biased negatively relative to the main chamber (the anode), which was at ground. This caused the discharge current to flow across the strong magnetic field to the anode. The primary electrons emitted from the cathodes were confined longitudinally by the electrostatic sheaths at each end and therefore permitted higher ionization efficiency than in a straight arc. The density, temperature, and potential profiles shown in Fig. 44 indicate a fairly uniform plasma suitable for experiments, but the plasma was subject to a high level of turbulence, as shown by the streak camera pictures of Fig. 45. The cause of the noise was not known at the time, but it is clear that such reflex discharges cannot possibly work without some sort of anomalous diffusion, since the electrons carrying the discharge current in such reflex or PIG (Phillips Ionization Gauge) discharges must cross the magnetic field to reach the anode. That the inward radial electric field excites a strong **E** × **B** instability in a partially ionized plasma was later pointed out by Al Simon[29], but the theory came too late.

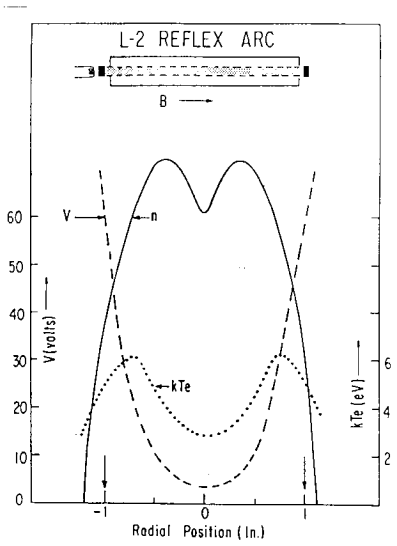

Fig. 44. Density, floating potential, and temperature profiles in the L-2 reflex arc (Ref. 30).

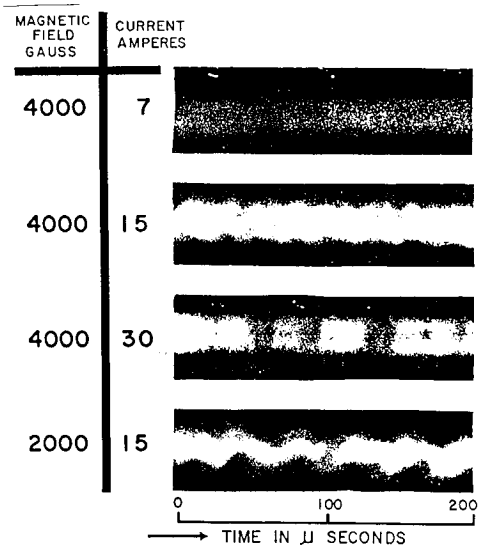

Fig. 45. Streak camera pictures of the reflex arc instability (Ref. 30).

The basic experiments that were planned could not be carried out, and two years of data on the operation of the discharge could not be explained, and therefore could not be published except in preliminary reports[30] By the time theoretical understanding of the **E** × **B** instability enabled us to design a discharge that would be free of it, the Q-machine had been invented, and there was no longer a need to do so.

However, all was not lost. By assuming a Bohm diffusion rate, we could solve the discharge balance equations and predict the observed radial potential profile, as shown in Fig. 46[31]. This much understanding was sufficient for PMT, Inc. to manufacture a reflex arc source for optical coatings, and for Bob Conn's group to use the reflex arc as a high-density source for the PISCES program. Fig. 47 shows a diagram of PISCES-A and Fig. 48 the oscillation level in it[32]. When used for for testing fusion materials and divertor designs, the basic instability of the plasma is of little importance. When used for studies of edge-layer physics, however, the PISCES machines would benefit by replacement of the reflex arc by a more stable source, such as the helicon source we will mention later.

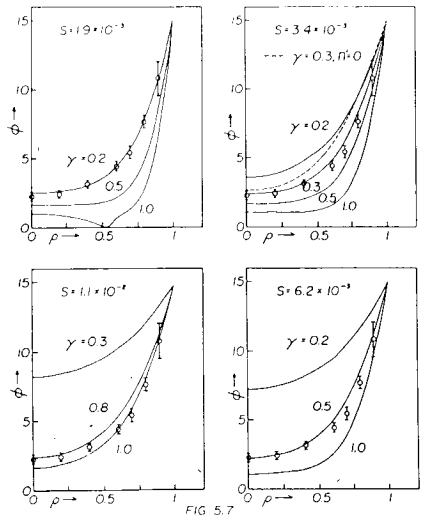

The L-2 machine was also used for an experiment on beam-plasma interactions. A 2-A, 20-kV electron beam from a Varian microwave tube was injected through a hole in one of the cathodes. Though many interesting effects were observed[33], none of them agreed with any known theory. Again, we were ahead of our time. I learned an early lesson in that experiment which I convey yearly to my students: Always learn to walk before trying to run. I should have started with a weak beam and worked near the threshold.

Fig. 46. Theoretical and measured potential profiles in the reflex arc. (Ref. 31).

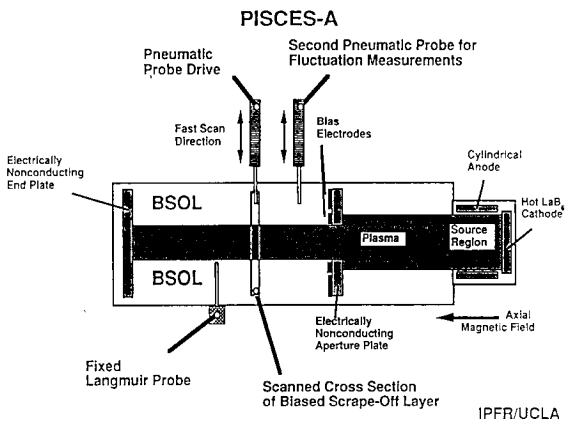

Fig. 47. The PISCES-A reflex arc (Ref. 32).

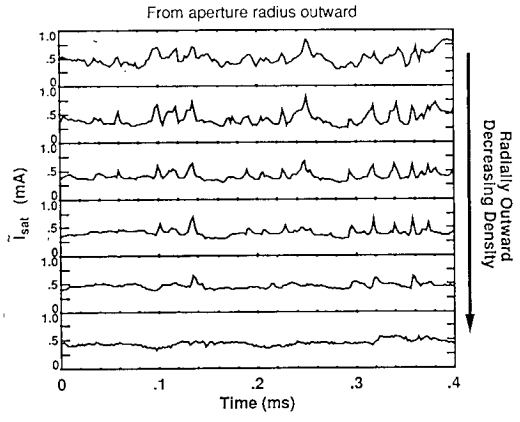

Fig. 48. Fluctuation level in the PISCES-A reflex arc (Ref. 32).

2. Edge stabilization of drift waves. Converting the L-2 reflex arc into a Q-machine was relatively simple, since we already had hot cathodes. We changed from 4" diam, 0.25" thick tungsten plates to 2" diam, 0.5" thick ones in order to have a more uniform surface temperature, and hence a more uniform potential distribution in the plasma. There were three large Q-machines operating at Princeton at the time, but a number of experiments were particular to the L-2Q device. By installing an insulated aperture limiter in front of the cathodes, as in Fig. 49[28], we were able to see the effect of applying different potentials V_c to the edge of the plasma. We found we could stabilize and destabilize drift waves this way. Fig. 50 shows the dc coupled probe current vs. time for various bias voltages. Below +4V, there was a turbulent spectrum of drift waves. At 4.0 volts, the plasma suddenly became completely quiet. As V_c was slightly increased, sinusoidal drift waves could be seen and studied at threshold. The waves grew with increasing bias, and eventually became nonlinear. The amplitude behavior with V_c given in Fig. 51[34]. There is a 2-V range of edge biases in which the drift waves are stabilized.

This observation was a clear indication of the strong effect of electric field shear on plasma stability. The problem was to prove it definitively. The first step was to measure the

radial electric field accurately. If one were to take radial profiles of floating potential, one would have to take the first derivative to get E_r, the second derivative to get E_r', and the third

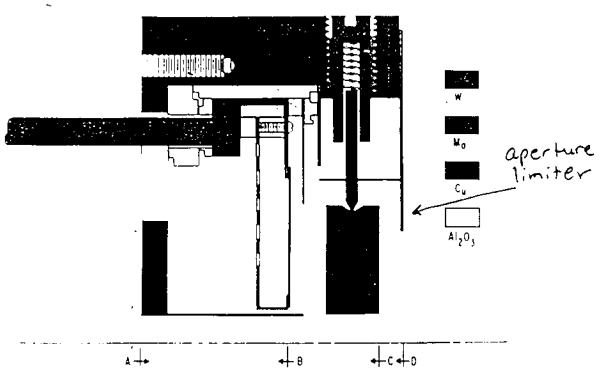

Fig. 49. Cross section of cathode structure with insulated aperture limiter and hole for harad core.

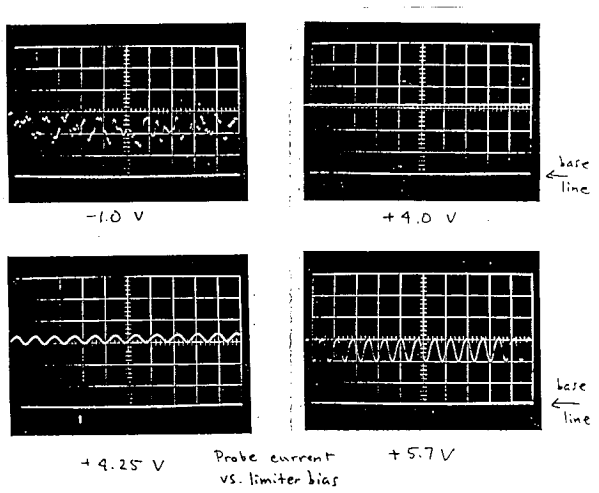

Fig. 50. DC coupled saturation ion probe current showing onset of drift waves as limiter bias is varied (Ref. 34).

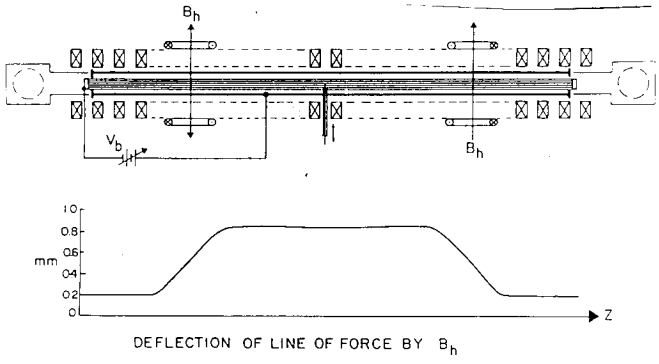

Fig. 52. Vertical field coil system used to displace the plasma (Ref. 35).

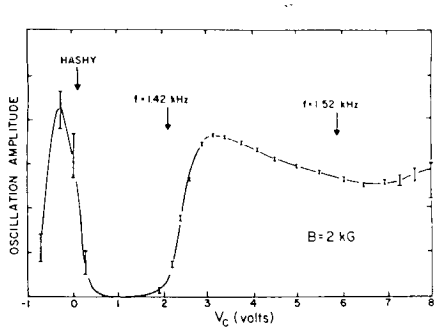

Fig. 51. Drift wave amplitude vs. limiter bias V_c (Ref. 34).

derivative to get E_r'', these terms being important in the Kelvin-Helmholtz effect.

It would be much better to measure E_r directly. We could do this by making a vibrating probe, which would continuously measure the potential difference at two radii separated by, say, 1mm. However, the design and construction of such a probe would have taken the Princeton engineers months, and there was also the danger that vibrations in the connecting cable could generate electrostatic charges. I decided to vibrate the plasma instead. This could be done by adding two sets of coils producing a vertical B-field, as shown in Fig. 52. By applying a 10-Hz sine wave to these coils, the plasma was moved up and down uniformly by a few mm at that frequency, and a lock-in amplifier tuned to the 10-Hz signal directly gave the electric field at the probe location. The frequency was chosen to be low enough to avoid exciting ion acoustic waves, but high enough to be usable with a lock-in amplifier. The coils, made of house wiring, were wound in one afternoon on wooden forms, and they were driven by two hi-fi amplifiers (stereo had not yet been commercialized).

The whole setup was done in one day, and the experiment worked like a dream. A typical electric field profile is shown in Fig. 53[35]. The wiggles near the axis were due to the hard core we had in the machine at the time (to be described in the next section), and the large E-field at the edge is due to the contact potential between the hot tungsten cathodes and the cold aperture limiter. In the body of the plasma, the E-field is linear with radius, corresponding to rigid-body $\mathbf{E} \times \mathbf{B}$ rotation of the plasma. *There was no noticeable change with limiter bias*, even though the oscillation amplitude varied wildly. Whatever was happening at the extreme edge we could not see accurately enough, but the electric shear at the maximum of the density gradient did not seem to be affected. This was a disappointing negative result, but we thought that at least the measurement technique was worth publishing. There is an interesting story behind why it was never published. Ken Rogers and I were working on this during his sabbatical, and he was put in charge of submitting this particular paper to Rev. Sci. Instrum. and seeing it through the refereeing process. Soon thereafter, he was made President of Stevens Institute of Technology. When the paper came back from the referee, it never saw the light of day in his office. So I have learned one thing about college presidents. They could care less about publishing another paper.

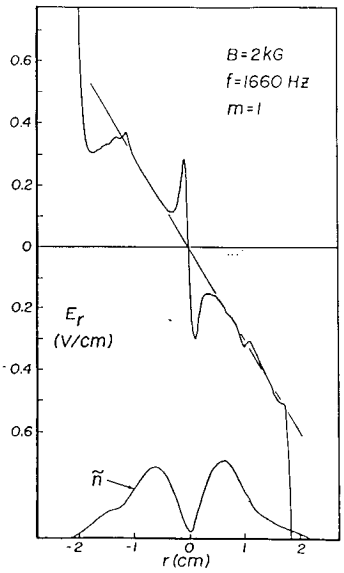

Fig. 53. Radial electric field profile measured with oscillating plasma (Ref. 35).

3. Shear stabilization of drift waves. Since we had a source of drift waves that was under control, it was natural to see how they could be stabilized by min-$\overline{B}$ and by shear. Let us

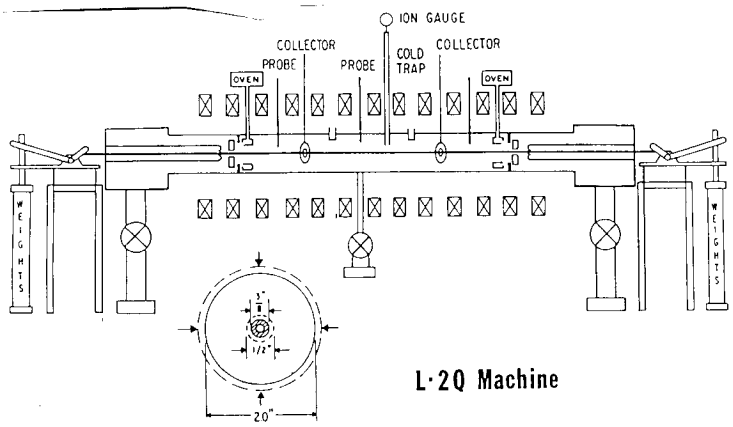

Fig. 54. Diagram of L-2 Q-machine with hard core.

consider the shear experiment. To impose magnetic shear, we decided to make 0.5″ holes in the cathode and filament assemblies and to string a water-cooled conductor through the holes to generate a B_θ field. When this problem was given to the engineers, they came up with the following solution: The hard core would be an aluminum tube, which had a better combination of weight and conductivity than copper, and there would have to be a cantilever system with lead weights to keep the tube straight as it heated and expanded during the current pulse.

Diagrams of the setup and the modified cathode assembly are shown in Fig. 54 and 55, and a photograph of the cantilever system is given in Fig. 56. When the hard core was pulsed, the lead weights sank; and after the pulse, they came back up. It was truly a Rube Goldberg device, but it worked. I think the physicists and the engineers at Princeton were amused at each other—the engineers that the physicists would want to do something like this, and the physicists that the engineers would come up with such a solution. The clearance between the hot tungsten cathodes and the water-cooled aluminum hard core was only about 0.5mm, so this was an accident waiting to happen...and it did. However, we recovered in time to make the APS deadline.

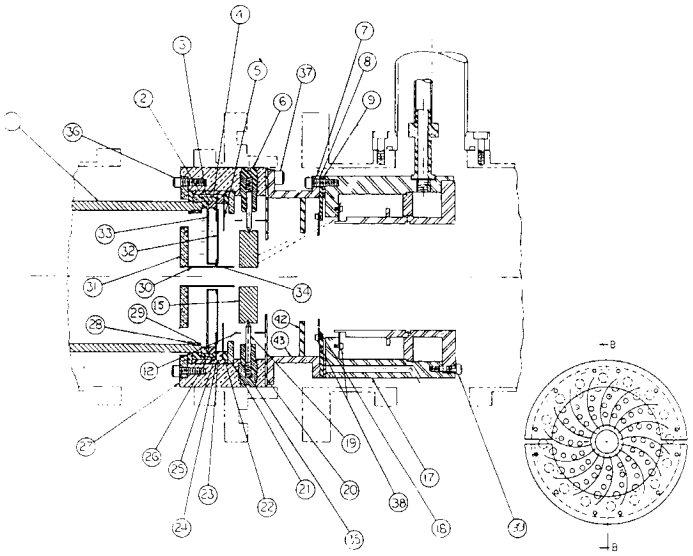

Fig. 55. Modified cathode assembly with hard core feedthrough on axis.

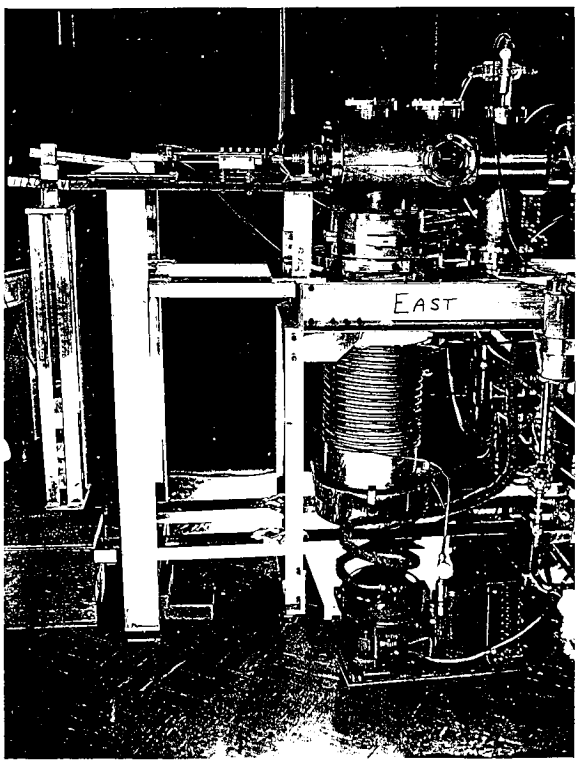

Fig. 56. Cantilever system for keeping hard core straight.

Fig. 57 shows the drift wave spectrum for various values of the current I_s in the hard core. It is clear that 2kA of current greatly reduced the drift wave turbulence. To see how the shear stabilization actually worked, my first student, Dave Mosher, probed the floating potential over a cross section of the plasma[35]. He found that the application of shear produced ripples whose wavelength decreased with increasing shear, as shown in Fig. 58. What was happening was that small temperature variations over the cathodes produced asymmetric potential contours in the plasma, giving rise to convective cells (Fig. 59). Plasma would $\mathbf{E} \times \mathbf{B}$ drift along these isopotentials and reach large radii rapidly. When the magnetic field lines are twisted by shear, these isopotentials are twisted into long spirals, shown in Fig. 60, which manifest themselves in the observed ripples. The twisting has the double effect of suppressing drift waves by squeezing them into a band narrow enough that ion viscous damping can be effective, and of increasing the length over which plasma must drift before reaching theoutside. Indeed, the plasma density measured at the highest shear was about half of that expected from purely classical diffusion (Fig. 61). Note in Fig. 61 the curve labeled n_{osc}. This is the density that would be expected if

all transport is by oscillatory diffusion. When the drift wave amplitude is greatly reduced by shear, the expected density is much larger than that observed, showing that most of the remaining loss is by convection rather than oscillatory diffusion.

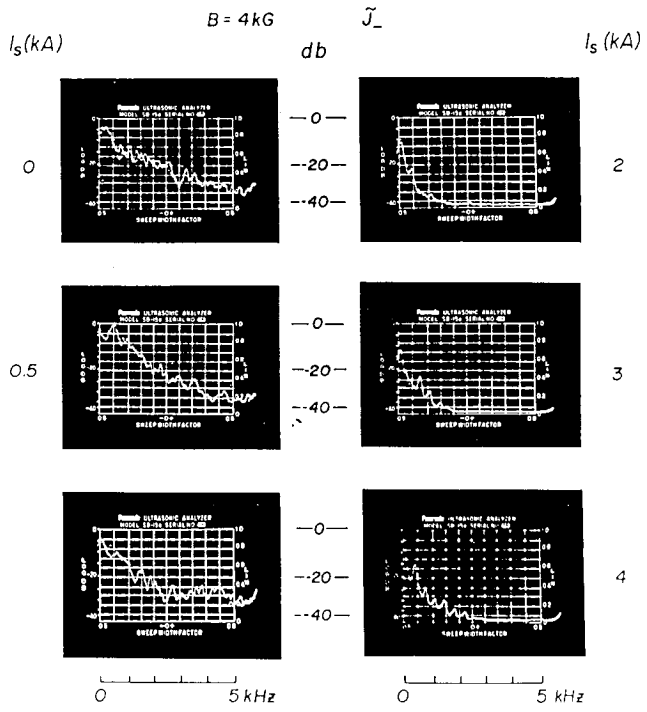

Fig. 57. Change of drift wave spectrum with hard core current (Ref. 35).

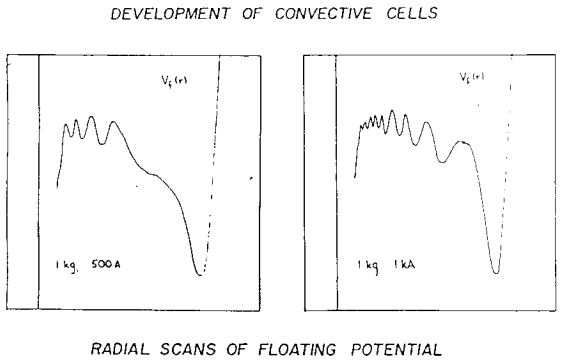

Fig. 58. Spatial oscillations in plasma potential in the presence of shear (Ref. 35).

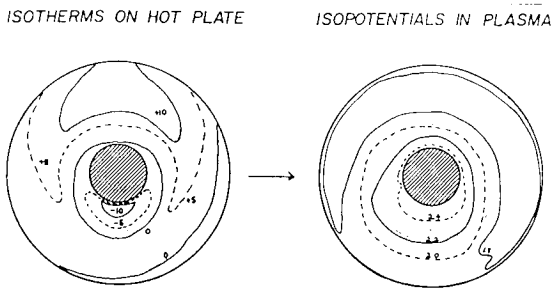

Fig. 59. Asymmetric isopotentials in plasma caused by temperature nonuniformities in cathode.

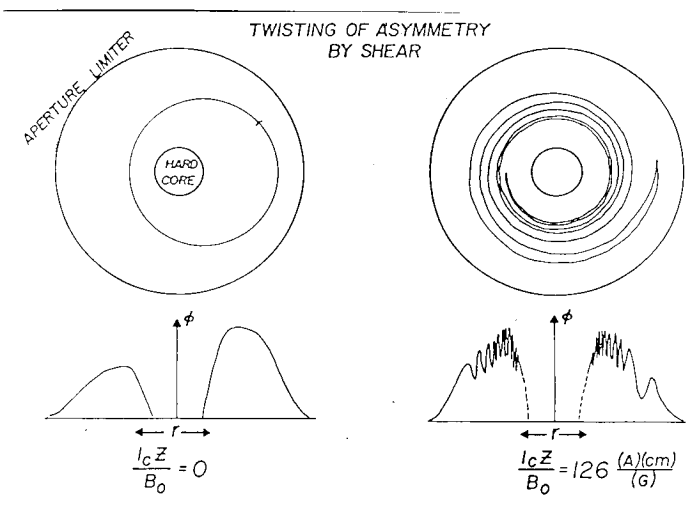

Fig. 60. Equipotential contours twisted by magnetic shear, providing the mechanism of shear stabilization (Ref. 35).

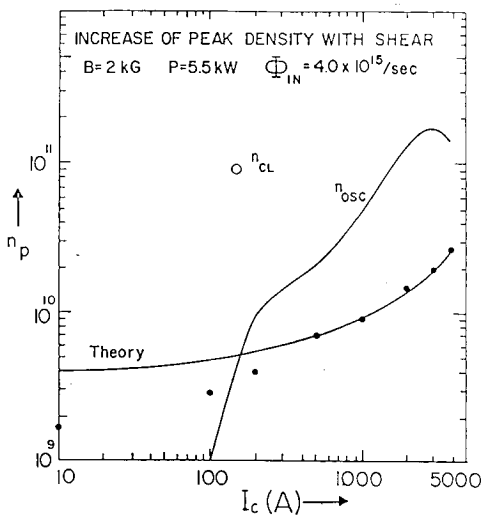

Fig. 61. Increase of plasma density with hard core current. The theoretical curve is based on the twisting of the equipotentials. The point n_c indicates the density there would be if transport were classical. The curve n_{osc} indicates the density there would be if all transport were due to oscillations; the measured oscillation amplitude is used (Ref. 35).

4. E × B instability in a beam-created plasma. We have seen that a transverse electric field of the right sign can excite the reflex-arc instability in a partially ionized plasma. The instability mechanism depends on the charge separation arising when the ions and electrons do not have identical **E** × **B** drifts because of the neutral drag on the ions. In fully ionized plasmas a small finite-Larmor-radius effect can cause drift-wave-like instabilities, but only when $k_\perp$ is finite. However, in weak magnetic fields in which the electrons are magnetized but the ions have Larmor orbits much larger than the plasma, the charge separation is so strong that even flute instabilities with $k_\parallel = 0$ can arise. This instability was discovered in the course of an experiment on chaos by Y. Sakawa[36] as part of his Ph.D. dissertation at UCLA. Fig. 62 shows the apparatus. In a uniform 160-G magnetic field, a weak electron beam (100 μA at 250V) is injected into 2×10^{-5} Torr of argon, ionizing a tenuous plasma of order 10^7-10^8 cm^{-3} in density. The negative charge of the beam causes a radial electric field of the proper sign for instability, as shown by the potential profiles of Fig. 63 for various beam currents.

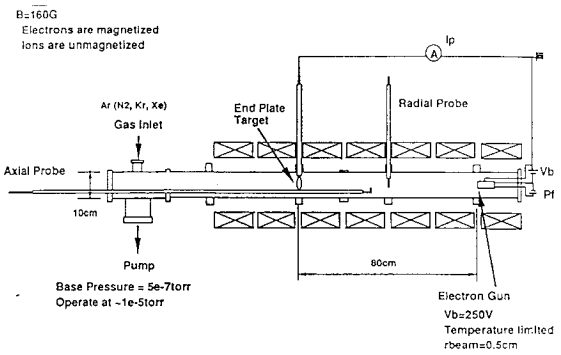

Fig. 62. Apparatus for weak beam-plasma experiment (Ref. 36).

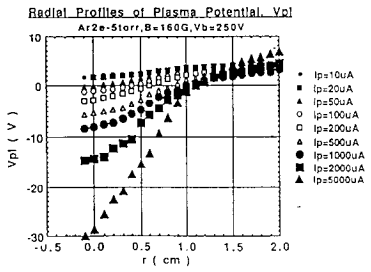

Fig. 63. Potential profiles measured in weak beam-plasma experiment (Ref. 36).

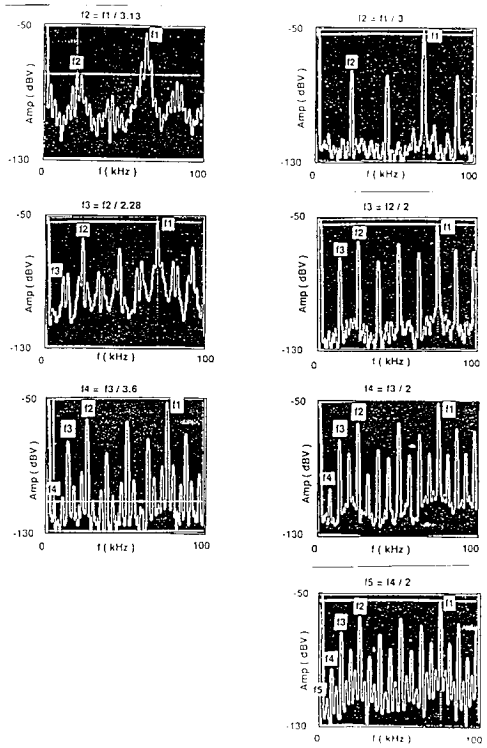

Fig. 64. Unstable oscillations generated by electron beam (Ref. 37).

Oscillations of two or more frequencies are seen; these are shown in Fig. 64 to lock into each other when they are harmonically related and generate turbulence through mode-coupling[37]. We are interested here in what causes the instability in the first place. The fundamental frequency is higher than the ion cyclotron frequency and much lower than the diamagnetic drift and **E** × **B** frequencies, thus eliminating all previously known instabilities. Here the small-but-finite ion Larmor radius picture is not at all appropriate, since the ions bounce in the radial potential well with orbits that are barely curved by the **v** × **B** force, as shown in Fig. 65. The finite curvature is all-important, because it causes a slow azimuthal drift of the ions, and this drift frequency is the only frequency the agrees with the observed one. By treating the ion orbits without a small-FLR expansion, we have found[38,39] that

indeed there should be a large growth rate in the experiment, and that the region of instability (Fig. 66) covers all but the weakest electric fields. This instability may be important in the weak-field discharges used in plasma processing and in strong electric field layers whose scale length is comparable to or smaller than the ion Larmor radius at the electron temperature.

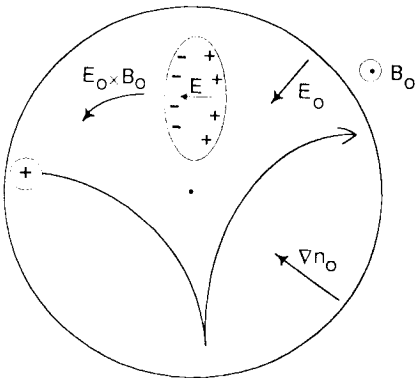

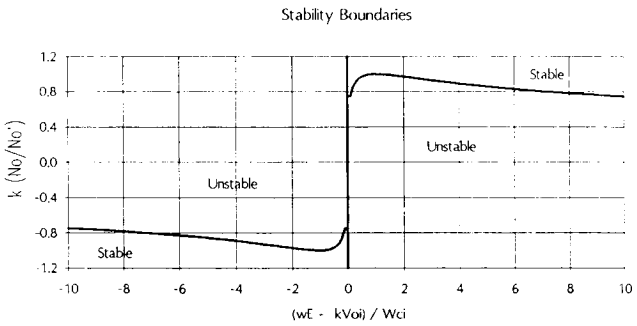

Fig. 66. Stability boundaries of the collisionless E × B instability with large ion orbits (Ref. 39).

Fig. 65. Mechanism of the modified E × B instability. The E × B rotation of the ions is much smaller than of the electrons, causing a charge separation wherever there is a positive density fluctuation. The resulting first-order E-field causes an outward drift when E_0 and ∇n_0 are both inward. This drift increases the local density at the expense of ∇n_0.

5. The tokamak H-mode. The discovery of the H-mode drew attention to the importance of transverse electric fields, and the difference in behavior of L-mode and H-mode discharges should give clues as to how the fields at the edge layer can affect plasma stability. Unfortunately, tokamaks do not provide a clean environment for basic experiments, since the magnetic field lines are not straight, and the plasma may have many charged and neutral species in the limiter region. In a uniform magnetic field, at least three mechanisms are involved with plasma stability in a transverse E-field: differential **E** × **B** drifts, Kelvin-Helmholtz effects due to electric shear, and drift wave effects due to pressure gradients. Note that the **E** × **B** effect can be strongly stabilizing in those regions where the sign is opposite to that in the reflex arc. These effects can be separated by proper experimental design, provided that the complicating factors of magnetic shear, trapped particles, etc. are eliminated. Consider the simple apparatus shown in Fig. 67. As discussed later, a helicon source can create highly ionized, quiescent plasmas in the 10^{13}-10^{14} cm^{-3} density range with just a few kilowatts of rf power. When put into a PISCES-type machine with a biasable aperture limiter, such a plasma can simulate the edge layer of the H-mode. In inertial fusion, we were able to isolate and understand the various parametric instabilities by doing specially designed experiments using specially tailored plasma sources. If basic experiments in magnetic fusion were still supported, the physics of the H-mode edge layer could be understood much better than it is now.

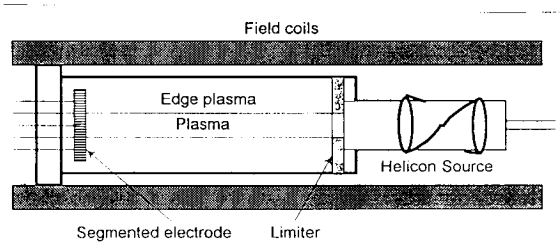

Fig. 67. Conceptual experiment using a helicon source to study tokamak edge layer physics.

electrostatically shielded helix (Fig. 71)[43]. Understanding and optimizing such plasma sources can be an interesting new direction for basic plasma research.

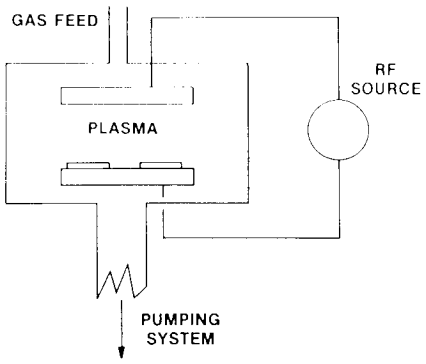

Fig. 68. Schematic of a parallel-plate capacitive discharge (Ref. 40).

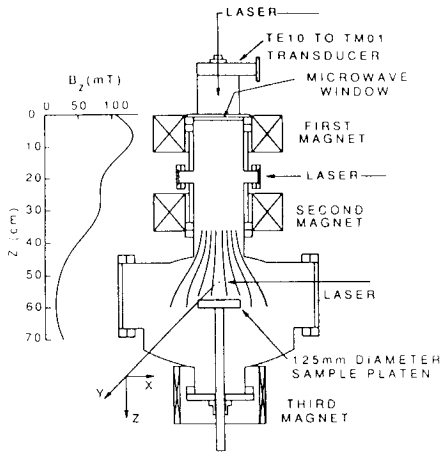

Fig. 69. Schematic of an electron cyclotron resonance source (Ref. 41).

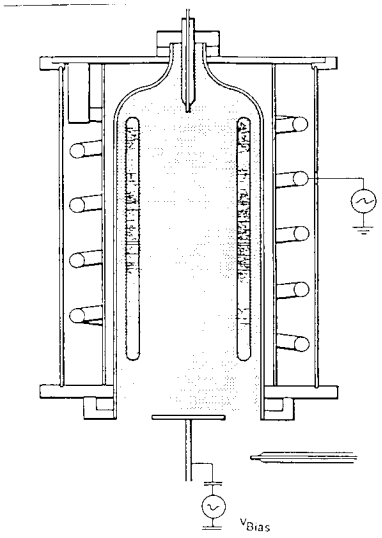

Fig. 71. Schematic of an inductively coupled discharge (Ref. 43).

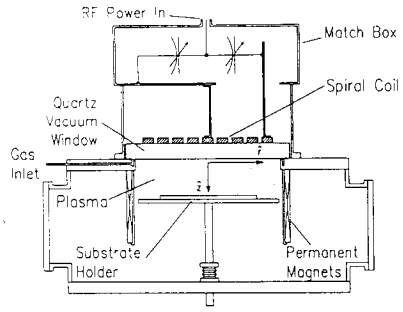

Fig. 70. Schematic of an RFI or TCP plasma source (Ref. 42).

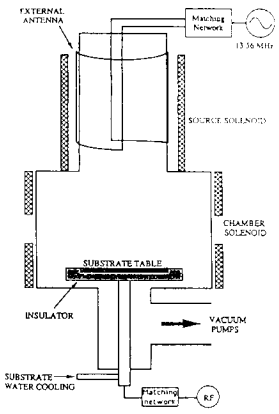

Fig. 72. Schematic of a helicon wave source (Ref. 47).

3. Development of the helicon source. At UCLA, we have been concentrating on the helicon source, which I got interested in because it has a higher ionization efficiency than any other source and has more flexibility. Helicon waves in plasmas are low-frequency whistler waves confined to a cylinder; they were first found by Peter Thonemann and his colleagues[44] in England. Later, Boswell[45] discovered in Australia that helicon discharges produced very dense plasmas. It was in Australia that I discovered Boswell and suggested that the ionization process might involve Landau damping[46]. Fig. 72 shows a diagram of a helicon source[47] applied to semiconductor etching or deposition, and Fig. 73 shows the apparatus we have used[48] the past few years to study the physics of helicon discharges.

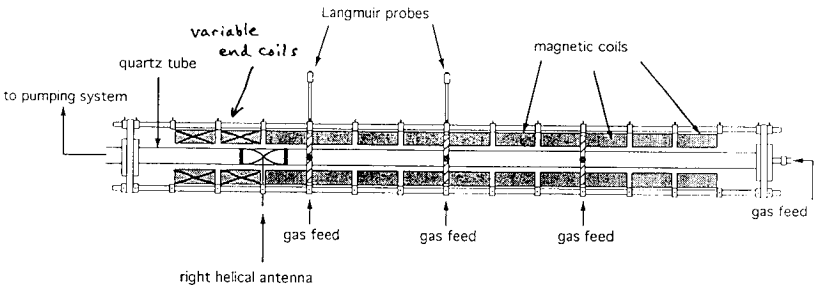

Fig. 73. Device for basic studies of helicon discharges.

Some of the possible advantages of helicon sources are as follows:

High density, high efficiency
Uniformity and quiescence
Low neutral pressure
Low B-field relative to ECR
No internal electrodes
Control of electron and ion energies
Remote operation, good access
Self-generated dc wafer bias

It has been fascinating and exciting research; we have verified theory in some cases and found unexpected effects in others. A few examples will suffice. Fig. 74 shows several antennas we have used and the peak densities obtained with them. The helical ones give higher densities and are supposed to excite m = +1 and -1 modes. We have computed the mode patterns for

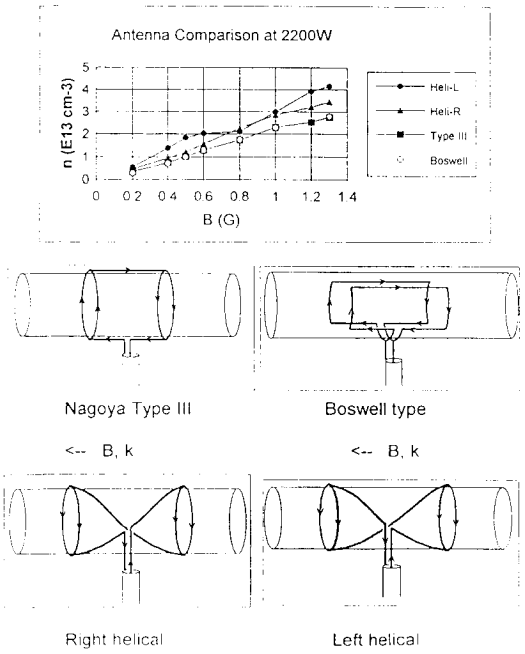

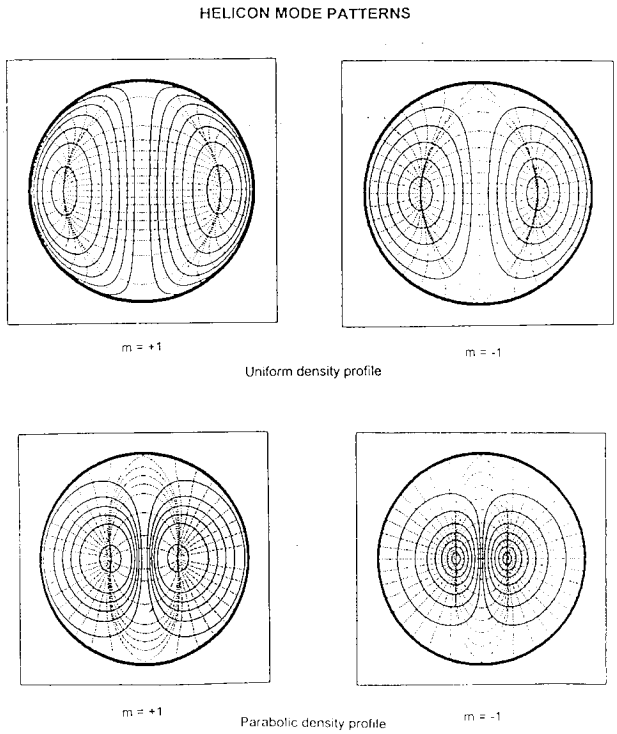

Fig. 74. Peak densities obtained with different helicon antennas vs. magnetic field (Ref. 48).

Fig. 75. Computed helicon mode patterns for right- and left-hand polarized modes (m = +1, -1) for uniform and parabolic density profiles (Ref. 49).

these modes in uniform and non-uniform density plasmas; the results are shown in Fig. 75. The m = -1 mode seems to concentrate the rf energy into a smaller volume near the axis, explaining why the left-hand helical (L) antenna gives the highest density. When we actually measured the mode patterns with a magnetic probe, however, we found that all antennas excited the m = +1 mode (Fig. 76)[49]. This discrepancy is still under study. When we reverse the

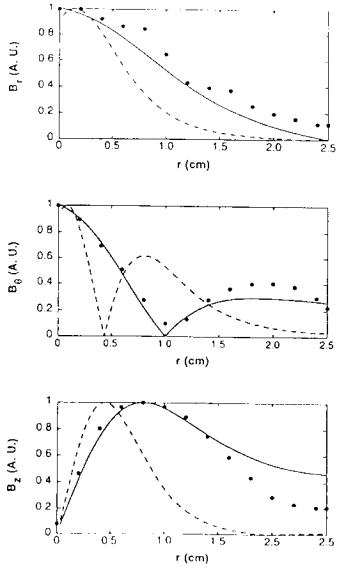

Fig. 76. Measured components of the wave magnetic field (points) compared with theoretical profiles for the m = +1 (solid line) and m = -1 (dashed line) modes in a helicon discharge (Ref. 49).

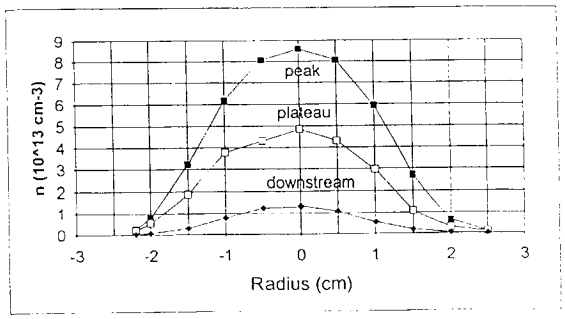

Fig. 77. Peak density in units of 10^{13} cm^{-3} in a helicon discharge. Gas depletion causes the lower curve marked "plateau".

end coils of the solenoid and place the antenna in a magnetic cusp field, we found a beneficial five-fold increase in axial density. After a long series of experiments, we believe that this is due to the magnetic aperture limiter effect, coupled with the destruction of the backward-going helicon wave. Fig. 77 shows the density profile at high pressure with the cusp field; note that the peak is nearly 10^{14} cm^{-3} even though there

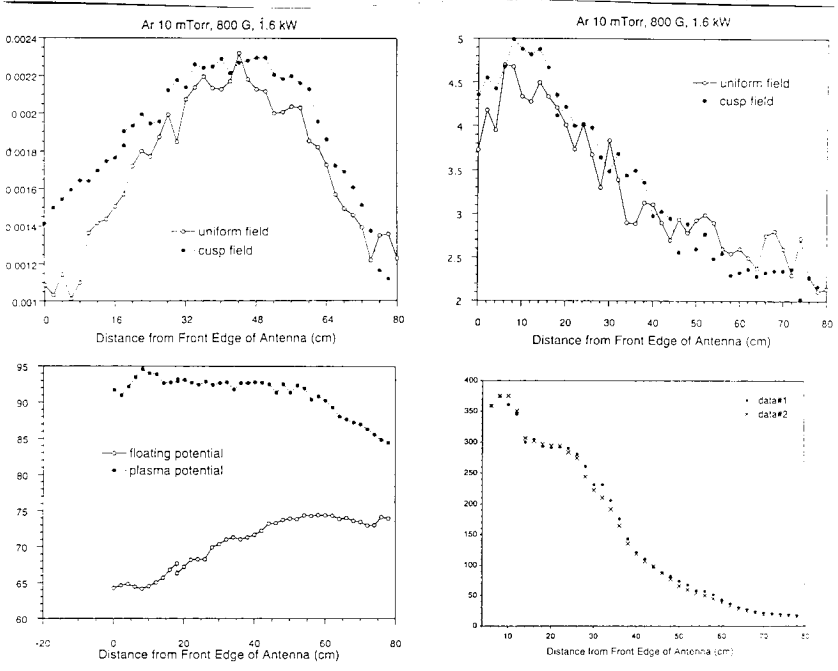

Fig. 78. Axial variations of density, electron temperature, space and floating potential, and ionized Argon light in a helicon discharge (data by I. Sudit.)

is no axial confinement. Recent measurements of the axial variations of density, electron temperature, space potential, and 488-nm Ar^+ light are shown in Fig. 78. It was at first surprising that the density should increase with distance away from the antenna. However, the other

curves show that KT_e drops, as it should, and therefore the density has to increase to maintain pressure balance. The floating potential also rose unexpectedly, but when it is corrected to the space potential, we see that the latter is flat, agreeing with the $E_{\|} = 0$ condition. The optical emission curve shows a falloff that is too slow to agree with the temperature profile, but if one assumes that metastables are created near the antenna and drift downstream, then the cold electrons there can ionize them and produce the observed curve. Studies of this kind show that basic plasma physics is still alive, and that industrial plasmas do not have to be treated in a rough and ad hoc fashion.

Conclusion. As plasma physics moves into the 21st century, I have no doubt that its main impact on society will come through its industrial applications, at least until fusion power becomes prevalent in the latter half of that century. Following the historical trend, as we have shown in this talk, the development of technological plasmas will no doubt be spearheaded by the invention of new plasma sources.

REFERENCES

[1] F. Boeschoten and F. Schwirzke, Nuclear Fusion **2**, 54 (1962).
[2] J. Malmberg and C. Wharton, Phys. Rev. Lett. **17**, 175 (1966).
[3] Wilcox, Baker, Boley, Cooper, deSilva, and Spillman, J. Nucl. Energy Pt.C **5**, 337 (1962).
[4] J.M. Wilcox, F.I. Boley, and A.W. deSilva, Phys. Fluids **3**, 15 (1960).
[5] R. Taylor, K. MacKenzie, and H. Ikezi, Rev. Sci. Instrum. **43**, 1675 (1972).
[6] R. Taylor, D. Baker, and H. Ikezi, Phys. Rev. Lett. **24**, 206 (1970).
[7] Y. Nakamura and I. Tsukabayashi, Phys. Rev. Lett. **52**, 2356 (1984).
[8] B.H. Quon and A.Y. Wong, Phys. Rev. Lett. **37**, 1393 (1976).
[9] B.H. Ripin and R.L. Stenzel, Phys. Rev. Lett. **30**, 45 (1973).
[10] R.L. Stenzel, Phys. Rev. Lett. **9**, 547 (1975); Phys. Fluids **19**, 857 (1976).
[11] R.L. Stenzel, A.Y. Wong, D. Arnush, B.D. Fried, and C.F. Kennel, AGARD-NATO Meeting CTP-138, No. 4-1 (1973).
[12] R.L. Stenzel, W. Gekelman, and M. Urrutia, Advances in Space Research **6**, 135 (1986).
[13] R.L. Stenzel, W. Gekelman, and N. Wild, Phys. Fluids **26**, 1949 (1983).
[14] C.L. Rousculp, R.L. Stenzel, and J.M. Urrutia, Phys. Rev. Lett. **72**, 1658 (1994); J.M. Urrutia, R.L. Stenzel, and C.L. Rousculp, Geophys. Rev. Lett. **21**, 413 (1994).
[15] W. Gekelman (private communication).
[16] N. Rynn and N. D'Angelo, Rev. Sci. Instrum. **31**, 1326 (1960).
[17] H. Hendel, T.K. Chu, and P. Politzer, Phys. Fluids **11**, 2426 (1968).
[18] R.W. Motley and N. D'Angelo, Phys. Fluids **6**, 296 (1963).
[19] A.Y. Wong, R.W. Motley, and N. D'Angelo, Phys. Rev. A **133**, 436 (1964).
[20] P. J.Barrett, H.G. Jones, and R.N. Franklin, Plasma Phys. **10**, 911 (1968).
[21] J.J. Turechek and F.F. Chen, Phys. Rev. Lett. **36**, 720 (1976).
[22] M.J. Herbst, C.E. Clayton, and F.F. Chen, Phys. Rev. Lett. **43**, 1591 (1979); J. Appl. Phys. **51**, 4080 (1980).
[23] B. Amini and F.F. Chen, Phys. Fluids **29**, 3864 (1986).
[24] B. Amini and F.F. Chen, Phys. Rev. Lett. **53**, 1441 (1984)
[25] C. Joshi, C.E. Clayton, and F.F. Chen, Phys. Rev. Lett. **48**, 874 (1982).
[26] F.C. Hoh and B. Lehnert, Phys. Fluids **3**, 600 (1960).
[27] F. Chen, J. File, and E.W. Lehmann, Project Matterhorn Tech. Memo 68, NYO-8071 (1959).
[28] F.F. Chen, Rev. Sci. Instrum. **40**, 1049 (1969).
[29] A. Simon, Phys. Fluids **6**, 382 (1963).
[30] R. Bingham, F.F. Chen, and W. Harries, PPL MATT-63 (1962); F.F. Chen, PPL MATT-249 (1964).

[31] F.F. Chen, Phys. Rev. Lett. **8**, 234 (1962).
[32] R.D. Lehmer, private communication.
[33] R. Bingham and F.F. Chen, Bull. Amer. Phys. Soc. 7, 151 (1962); F.F. Chen and R. Bingham, Bull. Amer. Phys. Soc. 7, 160 (1962)
[34] K.C. Rogers and F.F. Chen, Phys. Fluids **13**, 513 (1970).
[35] F.F. Chen, D. Mosher, and K.C. Rogers, Proc. 1968 IAEA Int'l Conf. on Plasma Phys. and Controlled Fusion Research **I**, 625 (1969).
[36] Y. Sakawa, C. Joshi, P.K. Kaw, F.F. Chen, ad V.K. Jain, Phys. Fluids B **5**, 1681 (1993).
[37] Y. Sakawa, C. Joshi, P.K. Kaw, V.K. Jain, T.W. Johnston, F.F. Chen, and J.M. Dawson, Phys. Rev. Lett. **69**, 85 (1992).
[38] F.F. Chen, Proc. Int'l Conf. on Plasma Physics (Innsbruck) **III**, 1789 (1992).
[39] F.F. Chen and M.J. Hsieh, Proc. Int'l Wksp. on Magnetic Turbulence and Transport (Cargèse, France), p.56 (1992).
[40] D.M. Manos and D.L. Flamm, *Plasma Etching* (Academic Press, 1989).
[41] N. Sadeghi, T. Nakano, D.J. Trevor, and R.A. Gottscho, J. Appl. Phys. 70, 2552 (1991).
[42] J. Hopwood, Plasma Sources Sci. Technol. **1**, 109 (1992).
[43] W.L. Johnson, Proc. 36th Techn. Conf., Soc. Vacuum Coaters (1993).
[44] J.A. Lehane and P.C. Thonemann, Proc. Phys. Soc. **85**, 301 (1965).
[45] R.W. Boswell, Phys. Lett. A **33**, 457 (1970).
[46] F.F. Chen, Plasma Phys. and Controlled Fusion **33**, 339 (1991).
[47] A.J. Perry, D. Vender, and R.W. Boswell, J.Vac. Sci. Technol. B **9**, 310 (1991).
[48] F.F. Chen and G. Chevalier, J.Vac. Sci. Technol. A **10**, 1389 (1992).
[49] M. Light, M.S. Thesis, UCLA (1994).